DUST STORM FORECASTING FOR AL UDEID AB, QATAR: AN EMPIRICAL ANALYSIS

THESIS

Kevin S. Bartlett, Captain, USAF

AFIT/GM/ENP-04-01

DEPARTMENT OF THE AIR FORCE
AIR UNIVERSITY

AIR FORCE INSTITUTE OF TECHNOLOGY

Wright-Patterson Air Force Base, Ohio

AFIT/GM/ENP-04-01

DUST STORM FORECASTING FOR AL UDEID AB, QATAR: AN EMPIRICAL ANALYSIS

THESIS

Presented to the Faculty

Department of Engineering Physics

Graduate School of Engineering and Management

Air Force Institute of Technology

Air University

Air Education and Training Command

In Partial Fulfillment of the Requirements for the

Degree of Master of Science in Meteorology

Kevin S. Bartlett

Captain, USAF

March 2004

AFIT/GM/ENP-04-01

DUST STORM FORECASTING FOR AL UDEID AB, QATAR: AN EMPIRICAL ANALYSIS

Kevin S. Bartlett, BS
Captain, USAF

Approved:

Steven T. Fiorino (Chairman)	2 MAR 04 date
Ronald P. Lowther (Member)	2 MAR 04 date
Daniel E. Reynolds (Member)	2 Mar 04 date

Abstract

Dust storms are extreme weather events that have strong winds laden with visibility reducing and operations limiting dust. The Central Command Air Forces (CENTAF) 28th Operational Weather Squadron (OWS) is ultimately responsible for forecasting weather in the vast, data denied region of Southwest Asia in support of daily military and humanitarian operations. As a result, the 28th OWS requests a simplified forecasting tool to help predict mesoscale dust events that affect coalition operations at Al Udeid AB, Qatar.

This research satisfies the 28th OWS request through an extensive statistical analysis of observational data depicting seasonal dust events over the past 2 years. The resultant multiple linear regression best fit model combines 28 easily attainable model outputs, satellite imagery, surface and upper air observations, and applies a linear transformation equation. The best fit model derived provides the end user with a numerical visibility prediction tool for Al Udeid AB that is verified against a seasonally divided and independent validation data set that yields an R^2 of 0.79 while maintaining < 800 m accuracy.

The operational significance of the summarized seasonal patterns and dust storm type offers operators within the region a quick synopsis of possible dust prone periods and duration of events; whereas the best fit model offers an easy-to-use, accurate dust forecasting tool. The fit model developed is ready to use and is expected to positively affect weather forecasts for flight operations at Al Udeid AB.

Acknowledgements

I would like to thank the many people who made this thesis work possible. First, I would like to thank my thesis advisor, Maj Steven T. Fiorino, for his technical assistance, and mentorship during this process. I would also like to express my gratitude to the other members in my committee, Lt Col Ronald Lowther and Mr. Daniel Reynolds, for the tremendous research and statistical expertise they provided.

This thesis would not have been possible without the help of Mr. Jeremy Wesley from the Air Force Weather Agency's technological division. Additionally, I would like to thank TSgt Kevin Wendt from the Air Force Combat Climatology Center for supplying data in many formats and CMSgt Salinda Larabee at the 28th Operational Weather Squadron for providing the initial regional dust data and operational forecasting rules of thumb. A special thanks goes out to Dr. Steve Miller and his staff from the Naval Research Laboratory, who provided me with the MODIS enhanced satellite imagery, and who answered the many questions I formulated in learning their products. Additionally, I would like to thank my sponsors at Air Combat Command who guided me with direction for the research and provided funding for necessary and invaluable trips.

I would like to thank my classmates for contributing scientific advice and levity during this research. Finally, I would especially like to thank my wife, children, and extended family who were extremely patient and understanding during the time dedicated to this work.

Kevin S. Bartlett

Table of Contents

Page

List of Figures

List of Tables

Table Page

DUST STORM FORECASTING FOR AL UDEID AB, QATAR: AN EMPIRICAL ANALYSIS

I. Introduction

Southwest Asia has been burdened with political unrest throughout modern history, an unrest that has earned the region a sometimes controversial, but stabilizing, United States military presence. The Department of Defense (DoD) and the Air Force continue to expand air, ground, military, anti-terror and humanitarian operations within this region and have strained current weather forecasting abilities. The diverse and ever changing missions require weather personnel to acquire extensive forecasting knowledge over this large and data denied geographical region to ensure mission safety and success.

Dust and sand storms comprise one of the more troubling meteorological aspects of Southwest Asia (SWA). Worldwide these storms can adversely affect millions of people, delay critical missions and effectively "grind operations to a halt" (Miner 2001). Greatly reduced visibility in the horizontal, vertical and slant range is the primary hazard affecting operations within dust storms (Miner 2001). Vast deserts engulf SWA whose many interior regions are riddled with infinite supplies of airborne lithometeors. Although dust can reduce visibility on any given day in this region, dust storms intense enough to significantly reduce visibility to affect daily operations are not an every day event. However, due to the frequency and severity of the dust storms that do occur, the myriad of health problems they cause, the aviation and ground travel hazards that occur and the delays they create; accurately forecasting the onset and impact of these storms is

continuing challenge to constantly rotating military personnel who deploy to the region for short periods then redeploy to their home stations.

Recently, the Air Force Weather Agency (AFWA) in a joint project with John Hopkins University's Applied Physics Lab released a dust specific, synoptic scale model. Together they applied the University of Colorado, Boulder Division's Community Aerosol Research Model from Ames/NASA (CARMA) and combined it with the AFWA Mesoscale Model 5th generation (MM5) model output and called it the Dust Transport Application (DTA) model. Under the premise of increased operational requirements, the Navy Research Lab (NRL) in Monterey, California, launched a two sided assault to also better forecast the dust storms in the same region. The Navy's aerosol models include the global NRL Aerosol Analysis and Prediction System (NAAPS) and a newer version of the Coupled Atmosphere/Ocean Mesoscale Prediction System (COAMPS™) with an aerosol prediction capability. Additionally, the Marine Meteorology Division at NRL devised a technique that enhances dust signatures on high resolution satellite imagery from the Moderate Resolution Imaging Radiospectrometer (MODIS) instrument onboard the Terra and Aqua polar orbiting satellites. All of these products have recently been developed and are now available to supply valuable synoptic and mesoscale dust forecast guidance for operators in this region.

The increased number of anti-terror and humanitarian missions staged from Qatar demand that a mesoscale forecasting technique be developed to enhance the current model outputs and reduce dust storm impacts on daily operations. The hypothesis of this research is that there are multiple and distinct environmental conditions foreshadowing dust storm origination that when coupled with high resolution satellite imagery and

numerical model output can more accurately predict the onset and severity of dust storms than either manual forecast analysis or modeling alone. Regularly measured surface and upper air conditions such as temperature, dewpoint, wind direction, speed and gusts, atmospheric pressure, and relative humidity can be monitored closely to identify common patterns and changes before the onset of dust storms. The goal of this research is to identify the environmental flags that have foreshadowed past dust events, match those flags with corresponding model outputs and satellite observations in order to develop a statistically sound mesoscale forecasting tool accurate to within 800 m for Al Udeid Air Base (AB), Qatar.

1.1 Background

Qatar is an oil and natural gas rich nation situated on a small peninsula about the size of Connecticut jutting northward into the Persian Gulf from the Arabian Peninsula. After the Iraqi invasion of Kuwait in 1990 and the regional repercussions, Qatari leadership slowly warmed to a stabilizing United States presence within the region. Recently, Qatari leaders offered the United States unrestricted military basing rights at Al Udeid AB and welcomed an increased and sustained US presence into central Qatar (Global Security 2003).

As a small peninsula, Qatar's immediate dust sources are limited, but due to its close proximity to extensive dust and sand source regions of the Arabian Peninsula, Qatar is plagued with intense seasonal dust storms similar to the surrounding areas. These dust

storms can adversely affect military and humanitarian operations generating from and returning to Al Udeid AB.

1.2 Statement of Problem

The Central Command Air Forces (CENTAF) 28th Operational Weather Squadron (OWS) forecasters located at Shaw AFB, SC are ultimately responsible for forecasting the weather and accompanying flight hazards for Southwest Asia. Since the Combined (Joint and Coalition) Central Air Operations Center (CAOC) base build up at Al Udeid has occurred in the past 2-3 years, the climatological weather records and forecasting techniques available for Qatar are restricted in scope and offer little guidance for the 28th OWS forecasters.

The 28th OWS's need to better forecast the onset and severity of sand and dust storms affecting Al Udeid AB, Qatar is a primary driving force behind this research. This study intends to fulfill the 28th OWS request for support by developing a mesoscale forecasting tool for Al Udeid AB, Qatar that spans the gap of the model limitations within this data sparse area.

1.3 Research Approach

Developing a mesoscale forecasting tool that accurately forecasts dust storms for

Qatar involves five distinct processes. First, seasonal and diurnal dust storm peaks and lulls are identified and understood by analyzing past regional studies. Next, surface and upper air data are collected from the Air Force Combat Climatology Center (AFCCC) spanning a period of record several years long from surrounding stations and analyzed for climatological and dust advection patterns. Then, the model output data are archived from NAAPS, COAMPS and DTA models and compared with surface observations and satellite imagery to determine the model's ability to forecast and detect dust storm events specifically affecting Al Udeid AB, Qatar -- which has been active for only the past 2 y. Then the dust data is grouped by location and the Al Udeid AB data is split evenly along seasonal lines. Finally, the resultant statistical analysis incorporating seasonal and diurnal patterns, surface and upper air parameters, as well as model and satellite interactions, are analyzed to show predictable wind speed and directional patterns and their immediate effects on reported visibilities at Al Udeid AB.

The results are then summarized as a semi-automated forecast decision aid that is statistically proven to predict known dust events. The resulting decision aid ultimately allows forecasters with limited regional weather knowledge to use the AFWA and NRL products to easily identify and forecast mesoscale dust storm development in Qatar in order to reduce the storm's adverse effects on daily operations.

II. Literature Review

2.1 Definitions

A dust storm is defined in the *American Meteorological Society's* (*AMS*) *Glossary of Meteorology* (Glickman 2000) "as an unusual, frequently severe weather condition characterized by strong winds and dust filled air over an extensive area. They usually arise suddenly in the form of an advancing dust wall that may be many kilometers long and a kilometer or so deep." The *AMS Glossary* continues to describe sand storms similarly as follows:

> A strong wind carrying sand through the air. In contrast to a dust storm, the sand particles are mostly confined to the lowest 5 meters, rarely rise more than 15 meters above the ground as individual sand grains and proceed mainly in a series of leaps, called saltation. Sand storms are best developed in desert regions where there is loose sand, often in dunes without much admixture of dust and are caused or enhanced by surface heating and tend to form during the day (Glickman 2000).

Air Force Manual (AFMAN) 15-111, Surface Weather Observations, defines dust and sand storms similarly to Glickman and provides guidance for reporting the severity of dust storms based on restrictions to visibility, "Report a dust/sand storm if the prevailing visibility is reduced to less than 1000 m,…report a severe dust/sand storm if the visibility is reduced to less than 500 m." The Kuwait dust studies by Safar (1980) also categorize dust and sand storms by the intensity reported. Safar found that when the visibility was reported < 1,000 m in winds at 9.5 m s^{-1} or greater, most stations reported a dust storm, but if the visibility dropped below 200 m, severe sand or dust storms were reported.

Dust and sand storms commonly occur simultaneously as larger sand particles obscure visibility in the lowest atmospheric layers and as smaller dust particles become lifted aloft through depths of many kilometers, effectively scattering incoming solar radiation and reducing visibility to distant objects. The expansive Arabian Peninsula (AP) deserts and surrounding complex terrain provide key dust storm ingredients such as limited precipitation, scarce vegetation, ample dust and sand sources as well as unstable, thermally mixed air providing essential vertical transport. Additionally, the persistent northwesterly winds and turbulent flows provide lift and the means to transport the dust-laden air deep into the atmosphere and well beyond the peninsula's sources. This research utilizes the definitions and timelines outlined by Wigner and Peterson (1982) as guidance to address dust and sand storms jointly since they are often difficult to observe separately. Therefore both airborne lithometeors are regarded as dust storm components from this point forward.

2.2 Topography and Source Regions

The Arabian Peninsula climate is classified as arid even though it is surrounded on three sides by water. The Red Sea lies to its southwest, the Arabian Sea to the southeast and the Persian Gulf to its northeast. Additionally the AP climate is significantly modified by its periphery of mountains. Jordanian and Syrian mountains lie to the northwest of Saudi Arabia, while to the southwest are the Al Hijaz and Asir ranges with peaks to 3,000 m, to the southeast are the Hadramaunt Mountains in Yemen, and to the northeast across the Persian Gulf lie the Zagros range in southern Iran. These

mountain ranges effectively block out precipitation from transitory extra-tropical cyclones that frequent the AP throughout the winter and spring. This lack of measurable precipitation, except along the coastal mountain regions, provides an inland ocean of sand and dust for the winds to feed upon. The mountains also tend to funnel surface winds from the northwest to the southeast across the peninsula year round.

The Arabian Peninsula and surrounding area provide multiple dust and sand source regions for any wind direction as depicted in Fig.1. Region 1 is known as the Mesopotamian source or fertile crescent encompassing the Tigres and Euphrates River deltas and flood plains where fourteen major dust sources have been identified (Wilkerson 1991). These sources are located within a complex river basin and tend to be marshy flat lands during the rainy winter months, but dry out quickly by late spring. This region is a primary source for dust storms into Kuwait, Coastal Saudi Arabia, Bahrain and Qatar.

Region 2 in northwest Saudi Arabia lies within a southern extension of the Syrian Desert known as the high desert of An Nafud or the Great Nafud (Bukhari 1993). This region has ample sand dunes, alluvial fans, dry washes and lake-beds to provide multiple point sources where many AP dust storms originate. Region 3 is known as the Ad Dahna Desert and connects the An Nafud in the north to the massive Rub al-Khali Desert that dominates southeastern Saudi Arabia. Oriented northwest through southeast, the Ad Dahna provides most AP dust storms with a continuous supply of dust as the storms flow southeast across the peninsula.

Finally within region 4, the Rub al-Khali Desert provides the last fuel for northwest originating dust storms before they drift into the Arabian Sea and eventually

dissipate. The Rub al-Khali is commonly known as the most arid and hottest location on the AP. Its vast sea of sand and dust provides a sizeable source region for all wind generated dust storms. It must be noted that additional source regions exist surrounding the AP but are considered beyond the scope of this study. This paper focuses on the 4 source regions identified as the providers of the majority of the dust storms that affect the study area of Qatar. With the topography specified, this review proceeds into the geological soil source studies and the wind speeds required to transport and lift dust in order to appreciably reduce visibility.

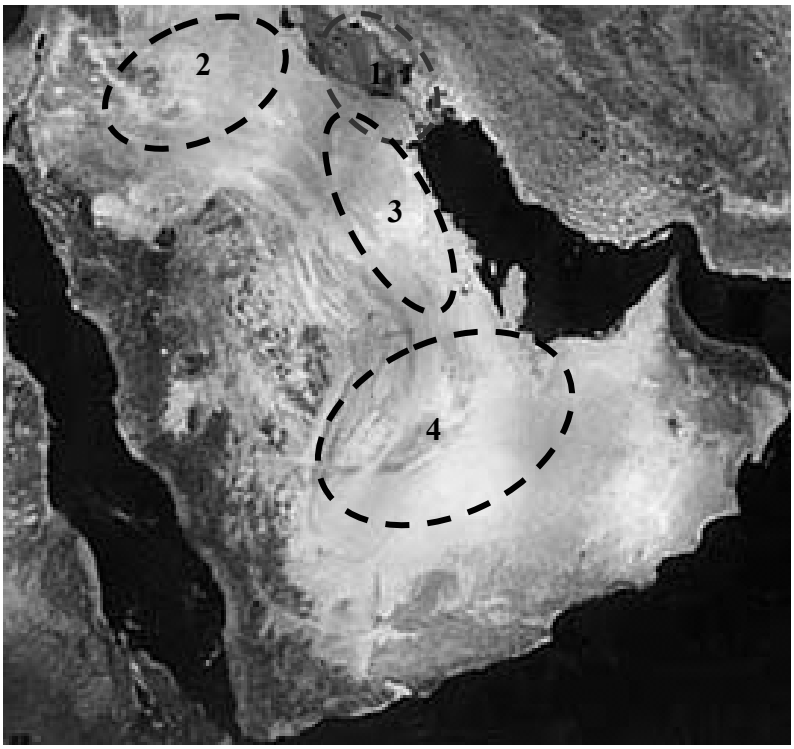

FIG. 1. Major dust and sand source regions. Graphic derived from the 28th Operational Weather Squadron (OWS) dust forecast training program. Region 1, Mesopotamian, Region 2, An Nafud Desert, Region 3, Ad Dahna Desert, Region 4, Rub al-Khali Desert.

2.3 Mobilization Studies

Clements et al. (1963) led a team of scientists from the University of Southern California into the deserts of Southern California with a large blowing fan to study the movement of sand and dust along various desert surfaces at controlled wind speeds. The following section summarizes their results and shows which soil type coupled with specific wind velocities will most likely produce dust storms.

Sand dunes were the first soil type the Clements et al. (1963) group investigated. Here they revealed a mere 6 m s^{-1} as the critical velocity required for suspension of finer sand particles (Clements et al. 1963). Additionally they noticed as the wind speeds increased, larger particles were moved and suspended easily within the air. They next studied a desert flat surface, which they described as a low-lying area within the desert floor where run-off water from surrounding higher terrain had settled and evaporated, but remained dominated by a sandy surface. They found that at 11 m s^{-1} the first significant amounts of fine sand began to move. When the wind speed increased to 15 m s^{-1}, significant sand, silt and clay particles lifted vertically and moved horizontally. As the study extended into dry washes, the team found that major drainage channels that carry ample winter rains, but later dry into the spring, deposit a significant amount of loose sand and silt along their paths as they flow. This plentiful medium to coarse sand provides a tremendous source for dust storms. They found the critical pickup velocity reduced to 10 m s^{-1} along the dry wash areas, whereas particles along loosely packed, sand desert roads required an even lower critical pickup velocity of 6 m s^{-1}. The team continued their work along an area of alluvial fans composed of coarse sands and covered

with a bounded crust that required a stronger critical velocity of 15 m s^{-1} to move larger particles which in turn dislodged the finer particles and suspended them (Clements et al. 1963). The final desert terrains investigated were the playas or dry lake beds with "crusted salts, clays and silts". They quickly learned that the crusted dry lake surface was "stable" and required a sustained critical wind of 15 m s^{-1} to move particles across the surface and effectively dislodge smaller imbedded particles (Clements et al. 1963).

The Clements et al. (1963) findings are summarized in Table 1. Additionally, it can be concluded from their intensive studies that the best sources for dust and sandstorms would be the extensive areas of dunes and dried out river washes, similar to those found in the Tigres and Euphrates River valley and the deserts of Saudi Arabia. Prospero et al. (1986) conducted further studies on naturally occurring dust at multiple field sites in Northern Africa and produced similar results. Prospero et al (1986) defined threshold velocity, another name for critical pickup velocities, as the minimum wind velocity required to initiate movement of surface sediments. When the threshold is reached, the wind's drag on the surface is strong enough to dislodge particles, set them into motion and lift them into the air at average velocities of 6.5 - 13 m s^{-1}. Threshold

TABLE 1. Summary of dust mobilization by wind speeds.

Horizontal wind speeds required to mobilize desert lithometeors

Desert Soil Source	Predominant Soil Type	Wind Speeds
Sand Dunes	Fine- Medium Sand	6 ms-1
Loose packed desert roads	Loose sand	6 ms-1
Dry Washes	Loose sand/Silt	10 ms-1
Desert Flat sand covered	Sand	11 ms-1
	Silt and Clay	15 ms-1
Alluvial fans-crusted surface	Medium-Coarse Sand	15 ms-1
Dry Lake beds and Playas	Crusted salts, clays, silts	15 ms-1

velocities vary greatly with each location based on source region terrain features, particle size, shape, moisture content, and soil composition. Most studies have shown that dust storms require minimum wind speeds greater than 5 m s^{-1} to mobilize dust, but Prospero et al. (1986) noted that larger scale blowing dust events require higher wind speeds of at least 11.5-13.5 m s^{-1}.

The independent Clements et al. (1963) and Prospero et al. (1986) studies resulted in similar criteria and allow the establishment of 10 m s^{-1} as a critical threshold of wind speed to lift dust into the air to reduce visibility in most cases. This correlates well with dust forecasting guidance from the 28th OWS for weather stations in their Area of Responsibility (AOR), which requires a minimum wind speed of 13 m s^{-1} to restrict visibility to 4800 m at most locations. It should also be noted that any anthropogenic activity across the previous mentioned soil surfaces in the vicinity of operational locations would loosen additional sediments and allow the particles to flow more freely at greatly reduced wind speeds.

2.4 Dust Storm Forcing Mechanisms

According to Wigner and Peterson (1982), natural dust suspension occurs when wind flows over loose, fine grained sand and soil and can be categorized according to flow type: synoptic versus mesoscale and duration.

1. Dust devils (limited aerial extent and occurrence)
2. Thunderstorm outflows (duration up to 30 min)

3. Frontal Passage (several hours ahead of cold front and approximately 1 h after passage of cold front)
4. Trough induced (4-8 h)
5. Associated with deep cyclones (12-36 h)

Lewis and Feteris (1989) found that man made dust suspension occurs when the soil is disturbed during heavy construction, agricultural cultivation, vehicular traffic or military maneuvers. Following these guidelines, this study addresses and expands upon the occurrence of dust storms, some of the operational hazards they present and establishes seasonal peaks within the study area.

Dust devils are small-scale whirlwinds of rotating columns of air created by differential heating of the earth's surface occurring on a micro-scale. They generally require dry soil surface, clear to partly cloudy skies, weak surface winds and air temperatures in excess in 27° C (Wilkerson 1991). The earth's surface is widely varied in slope, composition and color. Under the conditions mentioned above, these changes can create localized, rapidly rising motions near areas of stagnant, cooler air. The rising column pulls air into its core at the surface as it raises, twists and stretches with height, creating a localized whirlwind commonly referred to as a dust devil. Dust devils can reach extreme vertical heights in excess of 500 m, but are most likely observed to heights of 10-100 m. Once formed they move in erratic paths and slightly upslope (Wilkerson 1991). Dust devil winds have been estimated to range from 10 m s^{-1} to extremes of 25 m s^{-1}. Fortunately, dust devils are short lived, small in horizontal scale and dissipate within tens of minutes. The primary operational concern with dust devils is the unpredictable nature of their formation and forward motion. The localized wind shears

produced can adversely affect flight operations, landing or taxiing, and personnel. Dust devils tend to have a peak occurrence on the AP in the spring around April and early May, before the steady surface winds of the summer Shamal (SSH) develops.

The next level of dust event increases in scale and duration and happens within thunderstorm outflows. "Haboob" is a word derived from the Arabic word habb, which means to blow (Membery 1985), and is commonly found in studies to describe a strong convective downburst of strong winds accompanied by an intense but short lived dust storm. Haboobs can be micro or mesoscale events and can occur anywhere thunderstorms are common. They can flow tens of km ahead of the parent thunderstorms in the form of a gust front, as a wall of dust towering to 3 km with strong turbulent winds. Haboob dynamics are similar to United State's High Plains convective downbursts.

Desert surface conditions can be extremely warm and dry. When warm and moist coastal air is drawn onshore, it can contribute to developing rain showers and thunderstorms that can eventually produce rain reaching the surface. Often in desert environments the air below the cloud base is extremely dry. Falling rains tend to evaporate within the rain shaft, effectively cooling the air and ultimately increasing the downward wind and rain velocities. When the cold pool of air hits the ground, the edges of the cold air force air upward and outward churning and lifting sand and dust as it advances as depicted in Fig. 2. The leading edge of the created wall of dust will move ahead of the parent shower, causing a surface pressure jump, an increase and directional shift in near surface winds, and frequently, a drop in surface temperatures. Haboobs normally endure for 30 min to 3 h (Wilkerson 1991) but can extend beyond 6 h in rare

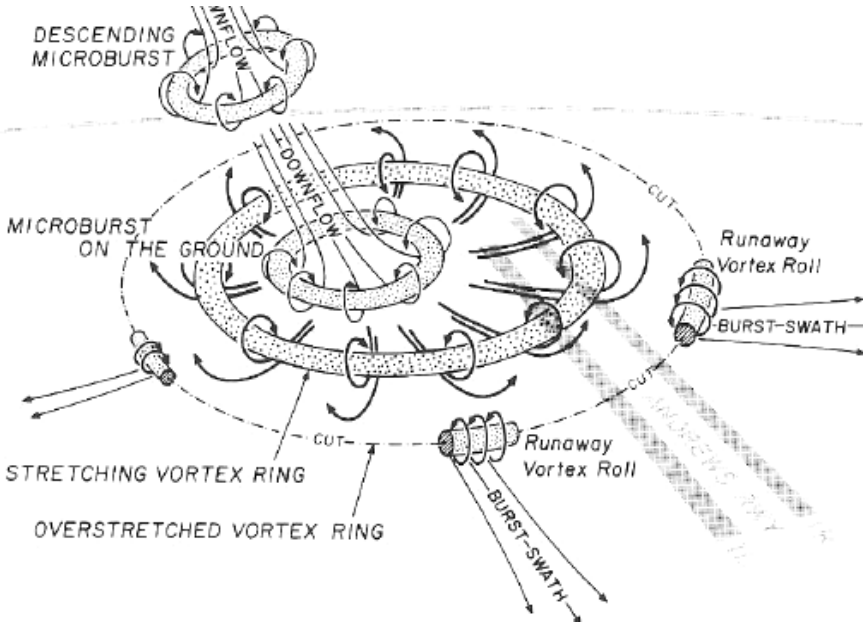

FIG. 2. Fujita's (1984) conceptual model of a microburst. Shows turbulent motions required to lift dust near the edges of the outflow.

instances (Membery 1985). Reportedly they are most severe in April and May; however they can occur anytime rain showers or thunderstorms are present. Climatologically, they are least likely to occur in November. Haboobs can be induced along vigorous cold fronts during the winter and early spring that approach from the north, but their origin shifts as the thunderstorm genesis' shift to the east, south and southeast. A haboob's greatest threat to operations is the rapid reduction of visibility to as low as 50 m as reported by Membery (1985), strong low level wind shear and surface winds. They have average winds at 22 m s^{-1} but can produce stronger winds closer to the originating downburst where winds have been measured at speeds to 33 m s^{-1} in the deserts near Phoenix, AZ (Idso et al. 1976).

Continuing with Wigner and Petterson (1982) guidance, the next synoptic level

dust event is associated with extra-tropical cyclone frontal passages, which can be subdivided into two distinct dust producers, Aziab, and Shamal winds. Aziab, a Saudi Arabian term, is a prefrontal event defined by Siraj (1980). Aziab winds are strong, hot and dry southerly winds that can raise massive dust storms characterized by a tightened surface pressure gradient. Many times during frontal passage across the AP a secondary Khamsin low (Siraj 1980) develops along the advancing cold front from the northwest as in Fig. 3. As the low pressure gradient tightens against a pre-existing high pressure to the south, southerly surface winds increase dramatically and draw moisture in from the Red and Arabian Seas. These southerly winds induce upslope precipitation events along southern Saudi Arabia and Yemen mostly in the form of high based thunderstorms near

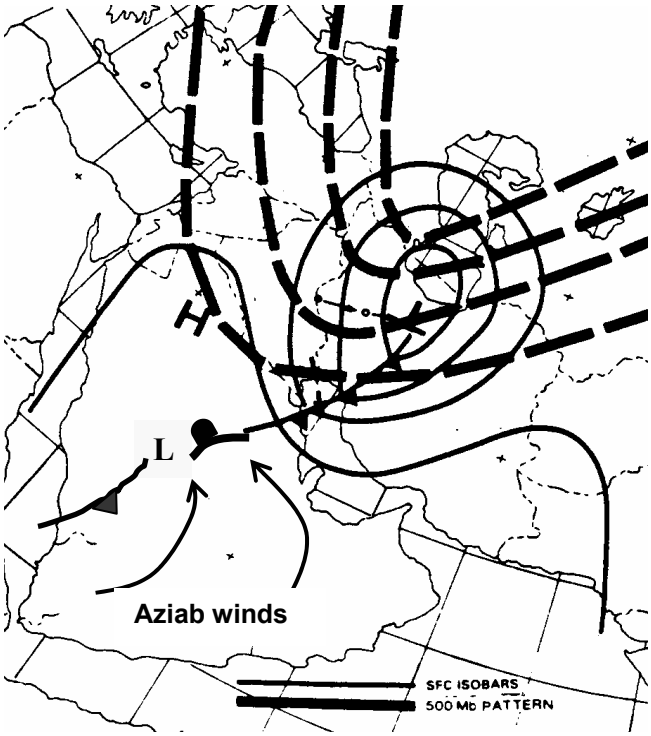

FIG. 3. Typical late winter Kamsin low development along a cold front. Parent extra-tropical cyclone shown with 500 mb and surface isobar pattern. (Adapted from Perrone 1979)

the coastal and mountainous regions, but this synoptic scenario also produces down slope, and drying winds into the AP interior. Aziabs primarily occur during spring, March-April, along the east coast of the Red Sea as the last of the strong, spring frontal systems affect the region (Siraj 1980). Climatologically, Aziab events are less frequent from May through September since fewer extra-tropical cyclones develop and migrate through the arid region.

The strength of an Aziab event is highly dependent on the location and intensity of the North African High pressure (Siraj 1980). The surface winds follow a typical developing low pressure prefrontal process. The winds start from east then shift to the south and increase in speed as the Kamsin low moves to the southeast across the AP (Siraj 1980). The winds ahead of the Khamsin dry and warm to temperatures of 37-40 C as they flow across the desert at speeds reaching 15-20 m s^{-1} (Siraj 1980). Aziab winds tend to last approximately 24 h or up to 2 – 3 d in extreme cases depending on the system strength and speed of motion. The strong southerly surface winds can stir up dust and sand decreasing surface visibilities to 200 m in some cases (Siraj 1980). As the associated cold front passes, temperatures cool and the winds transition to the northwest as Shamal winds. Surface visibilities can remain poor in northwesterly winds as velocities remain strong until the Kamsin low moves off the AP and away from its dust source. Aziab winds can also occur with more or less dramatic weather events such as strong upper level troughs or tropical cyclones.

The second synoptic scale wind is the Shamal, which means north in Arabic (Membery 1983). Shamal winds are derived from the prevailing northwesterly wind that flows across the AP year round. Rao et al. (2001) classified a Shamal wind event as

winds that flowed from a north to northwesterly direction and exceeded 8.5 m s^{-1} for at least 3 h throughout a 24 h period. The 3 h duration is critical in keeping the suspended dust aloft and is noted within the 28th OWS rules of thumb whereby occasional wind gusts to this wind speed will not produce enough dust to reduce visibilities significantly. There are two distinct Shamal seasonal patterns due to specific dynamical processes with one occurring in the winter and one in the summer.

This review first focuses on the winter and early spring Shamals that are associated with the passage of a distinct cold front. In recent studies about Qatar, Rao et al. (2001) characterized the winter Shamal season as one that begins in November and ends in March. His studies summarized 28 y of data focused on Qatar and showed that 26% of Qatar's Shamal days occurred within this period. Rao et al. (2001) as well as Perrone (1979), Safar (1980) and Wilkerson (1991), noted that winter Shamal dust events were the most intense in horizontal and vertical extent. The turbulent nature of the cold frontal boundary, coupled with high wind speeds, mix the dust to phenomenal heights up to 5 km (Wilkerson 1991). After passage, the strong post-frontal wind speeds can vary from 8-15 m s^{-1} and gust to 25 m s^{-1} which can reduce visibilities down to 0 m (Wilkerson 1991). These adverse conditions can occur during two different synoptic scenarios that drive winter Shamals. The first is coupled with a slower moving 500 mb pattern and a semi-stationary surface front that allows a Kamsin low to develop along the boundary and drift slowly east and northeast lasting 3-5 d as seen in Fig. 3. The second is associated with a standard mid-latitude cold frontal system with strong pressure gradients that progressively move across the AP and endure for 24-36 h and can be found in Fig. 4.

In contrast, the summer Shamal (SSH), commonly called "wind of 120 days," is a result of a seasonal semi-permanent high pressure in the Mediterranean region interacting with the summer monsoonal trough extending out of SW Asia and into Saudi Arabia and consequent surface heat low near Kuwait as in Fig. 5. Intense solar radiation into the deserts of the AP and SWA enhance the strength of the monsoonal trough and SSH from late May into early July (Membery 1983). This induced lower pressure amplifies the pressure gradient force from the Mediterranean Sea to the Arabian Sea creating sustained northwesterly winds for extended periods. Daily SSH winds can average 7 - 13 m s^{-1} during this period. The intense heating of the desert surface during the day turbulently mixes air and small dust particulates upward to heights approaching 3 km (Wilkerson 1991). As the horizontal winds increase they push the dust across the AP.

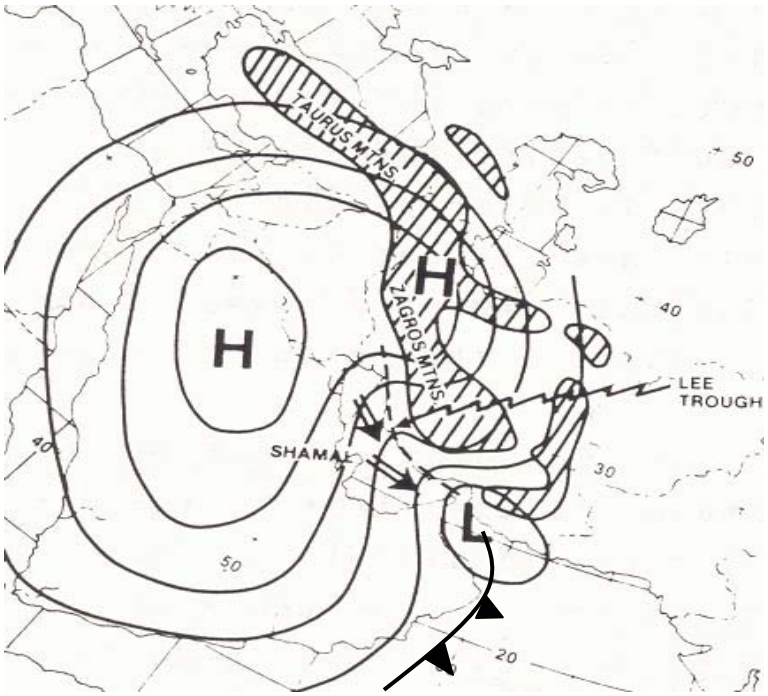

FIG. 4 Typical surface pressure gradient patterns during a 24-36 h winter Shamal. (Adapted from Perrone 1979)

Desert soils with limited vegetation are typically poor insulators; therefore the desert surface cools rapidly at night creating a surface based temperature inversion. This radiational inversion forces the stronger winds temporarily aloft and creates a stable region that reduces turbulent mixing of surface air and dust particles into higher altitudes overnight (Membery 1983). The inversion is one of the key processes in allowing the dust to settle as the surface winds decrease, consequently station visibilities tend to increase overnight at most reporting stations during the SSH (Safar 1980). When the sun rises and reheats the desert surface, the process is reversed as the stable inversion is mixed out by convective and thermal turbulence. Inversion breaking allows the strong

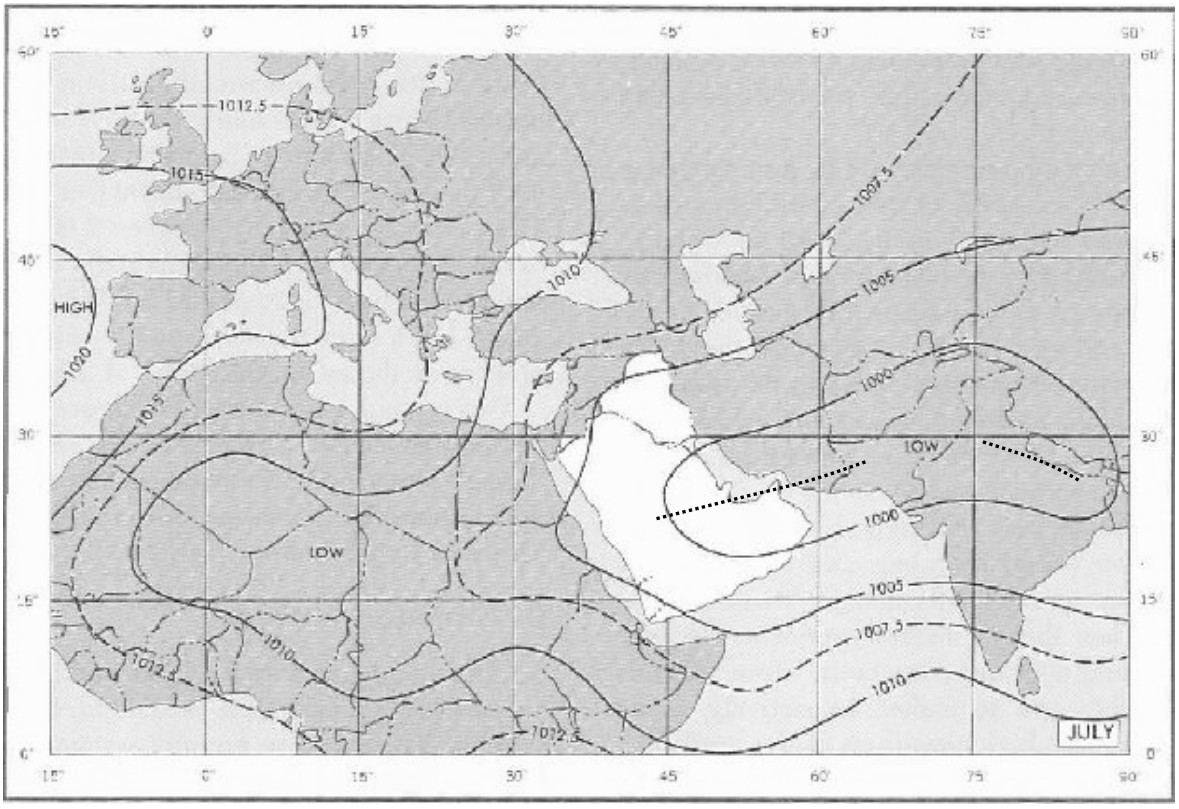

FIG. 5. July mean surface pressure patterns. Note the influences of the monsoonal trough from India through Africa and the Mediterranean ridging. (Adapted from the AFCCC graphics.)

winds held aloft by the surface inversion to return to the surface and reduce daytime visibilities dramatically at a rate proportional to the increasing wind speeds (Membery 1983). SSH events are typically longer in duration than winter Shamals and can last for several days or up to a week, but they normally do not produce the stronger winds and extreme visibility reductions to 0 m as is evident during some winter Shamals (Wilkerson 1991). In an earlier study Membery (1983), also found that due to the strong winds held aloft by the radiational inversion, there was strong wind shear through the inversions that posed a significant turbulence threat to smaller aircraft. These winds aloft are also a key ingredient in transporting the suspended dust across great horizontal distances.

The third synoptic scale dust event is trough or shear line induced. These low-level wind-shift zones normally form along washed out cold frontal boundaries during winter and spring with little upper level dynamics and weak surface convergence. As cold polar highs push frontal boundaries south out of Eurasia the northerly winds and colder air sometimes clash with easterly trade winds off the Arabian Sea (Wilkerson 1991). As the trough slowly moves south and east, convergent winds along the boundary lift dust into the air in the form of a weaker dust storm. Wind directions behind the trough are more northeasterly with speeds along the trough averaging 5-12 m s^{-1} and gusts to 15-20 m s^{-1} (Wilkerson 1991). Due to the weakened nature of most troughs, they tend to affect smaller areas with dust for 4-8 h (Wigner and Peterson 1982).

The final synoptic scale dust storm producer along the Arabian Peninsula is the tropical cyclone. These are relatively rare and normally only affect the southeastern coast of the AP. In a 70 y study, AFCCC (1970) found that 137 tropical cyclones were

observed in the Arabian Sea with 26 encroaching onto the AP with winds, rain and clouds. When tropical cyclones strike the southern coast of the AP, as they do approximately 1 time every 3 y, the storms are rapidly torn apart by surface friction and shearing upper level winds. They normally produce rains and high winds limited to the coast (AFCCC, 1970). Once inland, the cyclones have little remaining moisture, but sufficient winds to lift dust and create a cyclonic dust storm that can last 12-36 h (Wigner and Peterson 1982).

2.5 Past Forecasting Techniques

The AFCCC provided a study originally completed by the 2nd Weather Wing at Dhahran Air Base in September 1957 called, "Forecasting Visibility Restrictions Due to Dust at Dhahran Air Base in Summer". The study was designed to forecast advected dust that led to Instrument Flight Rules (IFR) conditions or visibility reduced to < 4800 m. Preliminary studies showed that the majority of summer visibility restrictions at Dhahran originated as advected dust from Iraq. Surface observations from Persian Gulf reporting stations such as Nasiriya and Basrah, Iraq and Abadan, Iran as well as upper air observations from Habbaniya, Iraq and Bahrain were used in the study. By hand plotting the data from the months of May through July from 1952 through 1953 the study identified a useable pattern of upper air 850 mb winds that transported the advected dust from the Iraqi fertile crescent of Region 1, identified earlier and located northwest of Dhahran, southeastward onto the Persian Gulf coastal region (AFCCC 1957).

A simplified version of the technique basically states that if there is no dust reported upstream, Visible Flight Rules (VFR) conditions ≥ 4800 m will prevail at Dhahran for at least 24 h. More importantly the study revealed that if dust was reported within Iraq and the 850 mb wind direction at Bahrain was from the northwest to north and the 850 mb wind direction at Habbaniya was from the northwest that dust would reduce visibility to IFR conditions for the next 24 h at Dhahran. Their methodology was simple yet very useful for Dhahran during the SSH. When independently tested during the summer of 1956 the study recorded a 76% success rate on the 1200 Zulu (Z) forecasts and an 82 % success rate on the 1800 Z forecasts which surprisingly was the same as a persistence forecast (AFCCC 1957).

The "Forecasting Visibility Restrictions Due to Dust at Dhahran Air Base in Summer" (AFCCC 1957) study resulted with the following general comments and hints of use for Dhahran, can be applied downstream from Iraq and are listed below:

1. The procedure is an objective aid in forecasting reduced visibilities due to the advection of suspended fine dust from Iraq.
2. Suspended dust may occur either with or without strong gusty surface winds and locally blowing sand.
3. IFR weather may result solely from blowing sand due to strong winds at Dhahran and this method gives no assistance in forecasting the wind speed at Dhahran.
4. When suspended dust is the only restriction to visibility, the visibility is usually lowest at approximately sunrise and usually becomes unrestricted by mid-afternoon.
5. When blowing sand also occurs with the advection of dust from Iraq, visibility often remains below 4800 m for the 24 h period. Visibility will most likely show slight improvement between 1700 and 2400 local time.
6. When blowing sand occurs alone, visibility is usually lowest between 1000 and 1500 local time.
7. Wind speed aloft is apparently of little consequence in applying this method; direction alone is the determining factor.

8. This method is intended primarily as an aid in preparing a 24 h Terminal Aerodrome Forecast (TAF) at 1200 and 1800 Universal Time Coordinated (UTC), and its applicability at other times have not been tested.

Many of the rules of thumb from AFCCC (1957) are used to derive the statistical predictors discussed later within this study in the methodology section.

The AFWA also addressed dust storm generation in a recently updated Meteorological Techniques Guide, AFWA Technical Note (TN) 98/002 (Mireless et al. 2002). The guide updated past studies and incorporated general rules of thumb, lessons learned and research results while addressing forecasting challenges specific to military meteorologists in three areas such as: surface weather elements, flight weather elements and severe weather. Under the Visibility Forecasting Rules of Thumb, Dry Obstruction section, TN 98/002 stated that after dust is already generated and held aloft, wind speed becomes important in the advection of the dust. "Dust may also be advected by winds aloft when surface winds become weak or calm" (Mireless et al. 2002). They found that the duration of a dust event is a function of vertical depth of the dust and the advecting wind speeds. Mireless et al. (2002) also noted that "forecasting dust generation is more difficult than forecasting the advection of observed dust into the area." The data within Table 2 summarizes the complex processes of dust generation and dust advection that the current research uses to devise the forecasting tool best suited for Al Udeid AB, Qatar.

2.6 Current Forecasting Techniques

Due to the additional operational needs in support of Operation Iraqi Freedom

TABLE 2. Conditions favorable for the generation and the advection of dust. (Adapted from AFWA/TN 98/002)

Parameter or Condition for Dust Generation	**Favorable for Dust Generation When**
Location with respect to source region	Located downstream and in close proximity
Agricultural practices	Soil left unprotected
Previous dry years	Plant cover reduced
Wind speed	≥ 15.4 m s^{-1}
Wind direction	Southwest through northwest (dust source upstream)
Cold front	Passes through the area
Squall line	Passes through the area
Leeside trough	Deepening with increasing winds
Thunderstorm	Mature storm in local area or generates blowing dust upstream
Whirlwind (dust devil)	In local area
Time of day	1200 to 1900 L
Surface dewpoint point depression	$\geq 10^{\circ}$ C
Parameter or Condition for Potential Dust Advection	**Favorable for Dust Advection When**
Wind speed	≥ 5.1 m s^{-1}
Wind direction	Along trajectory of the generated dust
Synoptic situation	Ensures the wind trajectory continues to advect the dust

(OIF) and Operation Enduring Freedom (OEF) in Afghanistan, the United States Air Force and Navy has stepped up efforts this year to field operationally tested aerosol transport models and dust specific satellite imagery enhancements. The AFWA in a joint project with John Hopkins University's Applied Physics Lab has taken the University of Colorado, Boulder division's Community Aerosol Research Model from Ames/NASA (CARMA) and combined it with AFWA MM5 model output and called it the Dust Transport Application (DTA). The DTA model is designed to forecast synoptic scale dust events within SWA as shown in Fig. 6. In an independent study, Barnum et al. (2003) discovered that the DTA can successfully forecast synoptic scale dust storm occurrences throughout SWA 61% of the time with a 10% false alarm rate. The AFWA rapidly tested and fielded operationally accessible DTA model outputs by creating an environmental worldwide web link on their Joint Air Force Army Weather Information

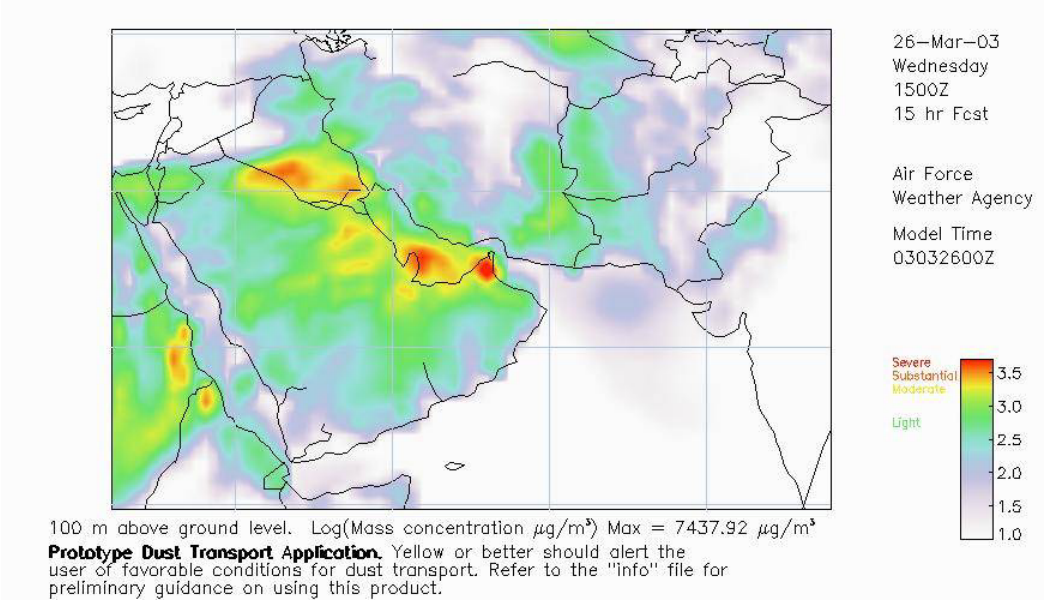

FIG. 6. Typical DTA output. 26 March 00Z run successfully forecasted a significant dust storm that affected Qatar on 26 March 2003. (Provided by AFWA/DNXT 2003)

satellite imagery and detailed regional dust event discussions. Additionally JAAWIN Network (JAAWIN). This site provides daily DTA model updates with forecasts out to 72 h, dust highlighted satellite imagery and detailed regional dust event discussions. Additionally JAAWIN provides a DTA tutorial link to train new users on the capabilities as well as the limitations of the DTA model outputs. The tutorial mentions that the DTA model's most pronounced limitation is the size of the model grid resolution compared to size of the terrain features and identified dust source regions.

Much of the DTA's successes of prediction can be attributed to the diligent work of Dr. George Ginoux and his staff at the Georgia Institute of Technology. His team utilized Advanced Very High Resolution Radiometer (AVHRR) and Total Ozone Mapping Spectrometer (TOMS) data to painstakingly map dust source regions from

Africa through China. Ginoux's identified sources represent the majority of observed regions, but due to the soil type sensitivity and horizontal scale limitations of the remote sensors, some of the source regions previously identified in this study are not reflected in the DTA model outputs (Barnum et al. 2003). Under-analyzed AP source regions result in a pronounced under forecast of synoptic scale dust storm events within the Saudi Arabian interior. Ginoux's dust source identification method identified Region 1, Fig. 1 well; therefore according to Barnum et al. (2003), the forecasting skill of the DTA model increases to an 81% success rate for areas downwind through Kuwait and along the Persian Gulf coastal region. The dust storm forecast success rates for synoptic scale systems are promising to operational forecasters in this region. However, though the DTA model has tremendous applications at the synoptic level, the 28th OWS forecaster's guides and tools for meso-scale dust forecasting in SWA are general and limited in scope.

In addition to the AFWA's modeling efforts, the Navy Research Lab (NRL) in Monterey, California launched a two sided assault on the dust storms in this region. The Navy's aerosol models include the global NAAPS and a newer version of the COAMPS with a meso-scale aerosol prediction capability. The NRL created a highly accessible aerosol website that allows the end user to select the world region of interest, the model of interest, NAAPS or COAMPS 4-panel output with a 48 h NAAPS and a 72 h COAMPS outlook and loop. The website also has links to current satellite imagery as well as archived model output.

The NAAPS model output as shown in Fig. 7 was developed with a global capability to analyze and model natural and anthropogenic aerosols. NAAPS combines remote aerosol measurements from worldwide surface based sensors with several

geostationary and polar orbiter remote sensing platforms that monitor daily aerosol fluctuations and Navy Global Atmospheric Prediction System (NOGAPS) weather forecasts to produce the regional and global scale aerosol forecasts. The NRL ingests data from many sources in countless spatial and temporal scales and there remain many

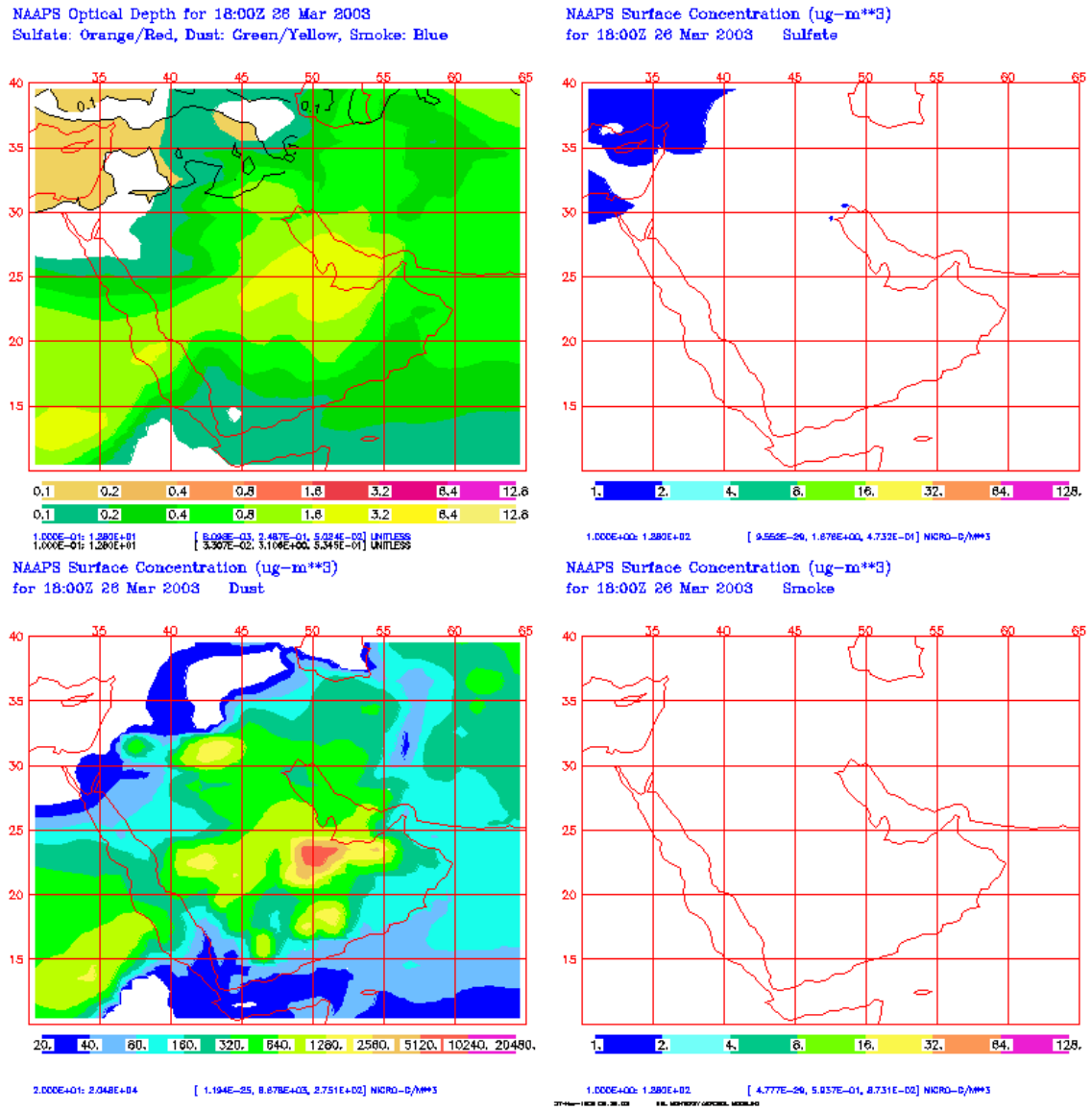

FIG. 7. Typical NAAPS output. 26 March 00Z run successfully forecasted a significant dust storm that affected Qatar on 26 March 2003. (Provided by NRL 2003)

challenges to overcome. Some of these challenges include but are not limited to determining the altitude of identified aerosols, identification and characterization of the source regions, conversion of synoptic observations to aerosol concentration and combining the data streams into common format (NRL 2003). Because of the scale of the challenges to the current NAAPS processing procedures, the previously introduced NAAPS outputs remain in the development stage, are not always available and are not operationally tested. However when available the NAAPS outputs can provide an additional valuable synoptic scale tool for dust forecasting in Qatar (NRL 2003).

The COAMPS mesoscale aerosol model output shown in Fig. 8 is a recent addition to standard Navy model outputs that started development in 1977 when COAMPS was designed as a short term, 72 h, meso-scale forecast tool for any region on the earth. Because the NRL has utilized COAMPS for so long, it is considered a reliable and stable model output that has many derivations and applications from the synoptic down to the micro-scale. Expansion of COAMPS into an aerosol transport platform was a natural progression of this meso-scale output, however the current aerosol model output has not been field tested and is provided to field units for additional dust forecasting guidance only.

Additionally, the Marine Meteorology Division at NRL under the guidance of Dr Steve Miller devised a breakthrough technique that rapidly downloads, reprocesses, and enhances dust signatures on high resolution satellite imagery from the Moderate Resolution Imaging Spectroradiometer (MODIS) instrument onboard the Earth Observing System (EOS) Terra and Aqua polar orbiting satellites. The enhancement process is limited to visible images and uses algorithms to combine infared and high

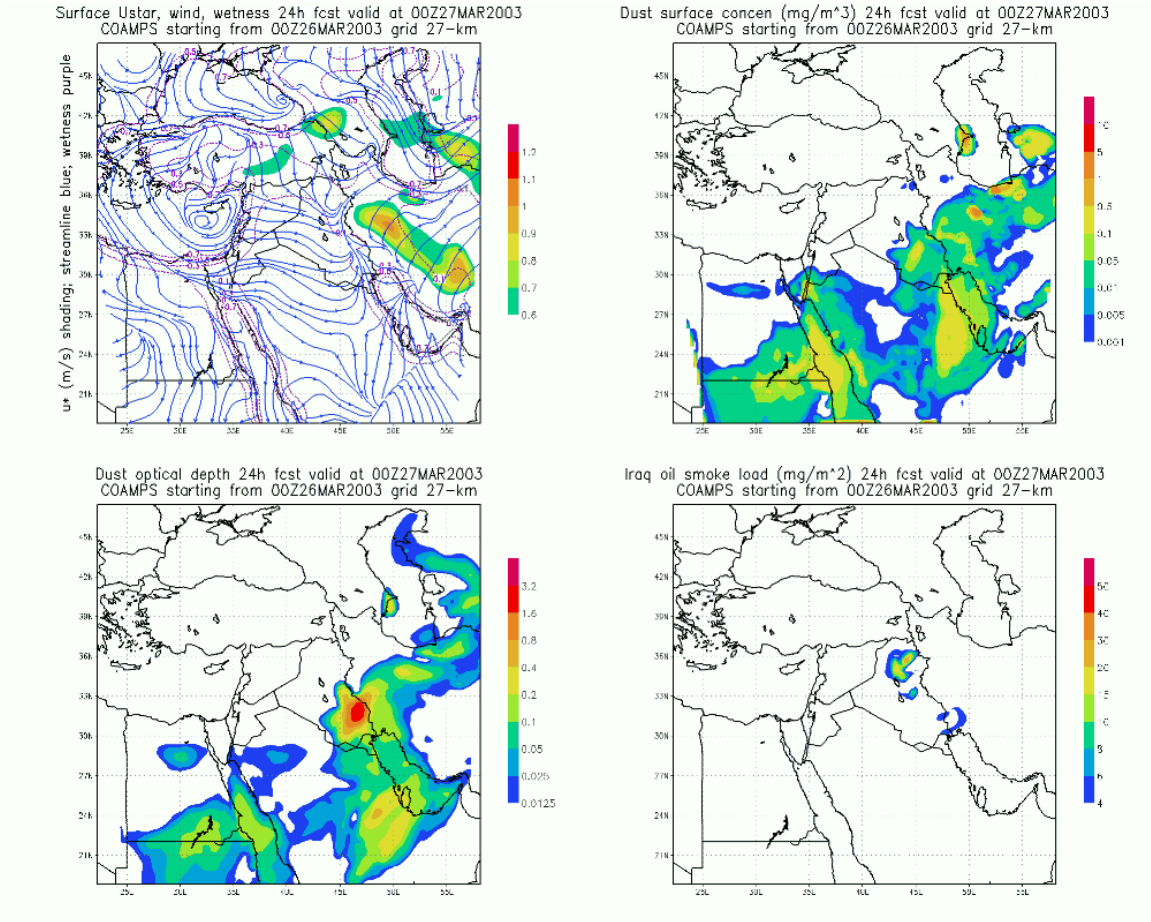

FIG. 8. Typical COAMPS output. 26 March 00Z run successfully forecasted assignificant dust storm that affected Qatar valid 27 March 2003. (Provided by NRL 2003)

resolution visible channels as well as false color enhancements to discern between cloud cover and surface based dust (Miller et al. 2003). The operational products are provided by the Fleet Numerical Model Operations Center (FNMOC) to the end user through a one-stop secure website known as "Satellite Focus" and shown in Fig. 9 (Miller et al. 2003). "Satellite Focus" provides, regionally focused images, looping capabilities, multiple atmospheric phenomena enhancements, forecasted satellite passes and product tutorials. The resulting satellite products have been operationally tested and have

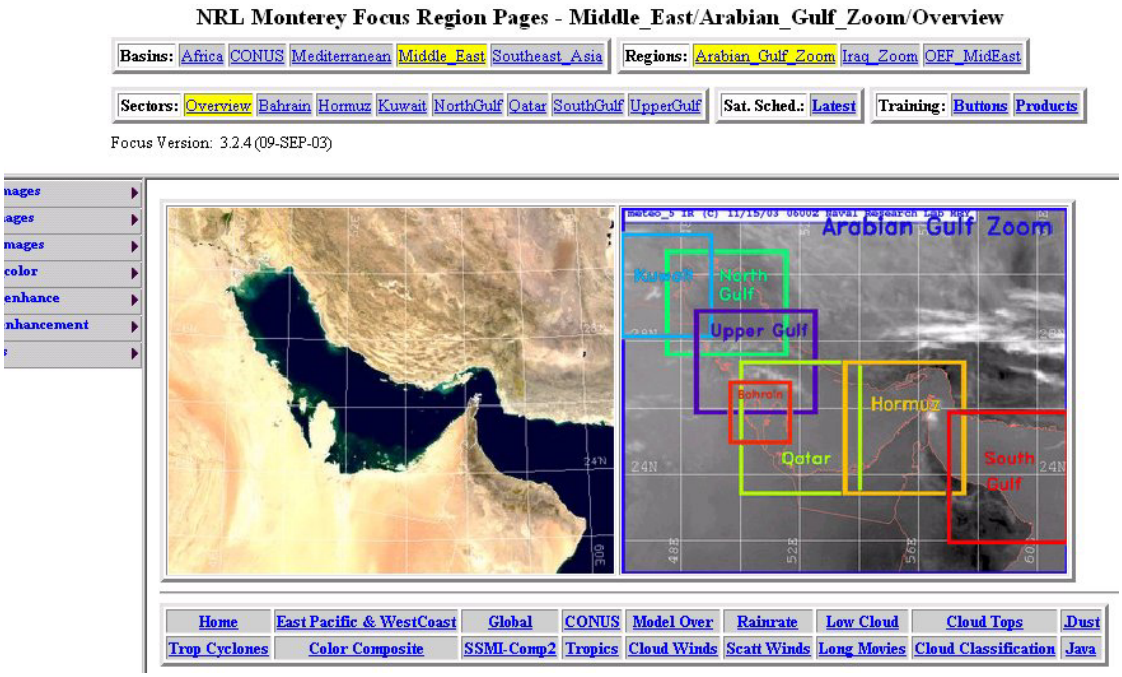

FIG. 9. "Satellite Focus" options menu. (Provided by NRL 2003)

successfully supplied valuable dust event enhancement imagery for operators in SWA supporting OEF and OIF (Miller et al. 2003). Perhaps most impressive are the color dust enhancement images as seen in Fig. 10; which though limited in temporal scale, clearly enhance dust events over land or water revealing major as well as minor dust events. These satellite download procedures and products have been under development since September 11, 2001 (Miller et al. 2003). The satellite products highlighted in Figs. 9 and 10 have been operationally tested and have successfully supplied valuable dust event imagery for operators in this region supporting OEF and OIF. As a final note, the FNMOC has been using all three NRL model and satellite images in conjunction with the AFWA DTA products mentioned earlier to discuss daily dust outlooks, areas of interest and model comparisons. These discussions are expected to be expanded to other

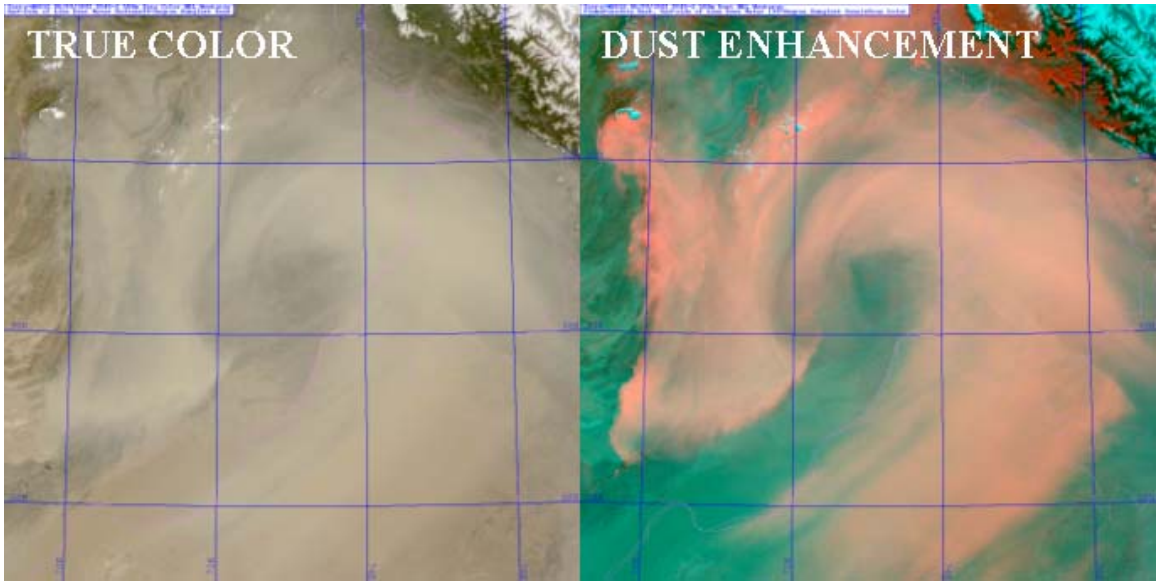

FIG. 10. High resolution true color MODIS imagery and dust enhancement imagery. (from Miller 2003)

agencies through secure FNMOC web channels with time (Liu et al. 2003), and suggest an operational release in the near future.

2.7 Regional Study Summary

With the current forecasting techniques addressed, this review focuses on summarizing some of the more recent regional dust studies completed. The three regional studies by Bukhari (1993), Safar (1980), and Rao (2001), encompass over 50 y of surface observations for Saudi Arabia, Kuwait and Qatar respectively. Figure 11 graphically summarizes the studies by highlighting patterns showing seasonal peaks of dust storms and Shamal winds beginning in March then increasing into June and July during the SSH. Bukhari (1993) compiled the Saudi Arabian Meteorological and

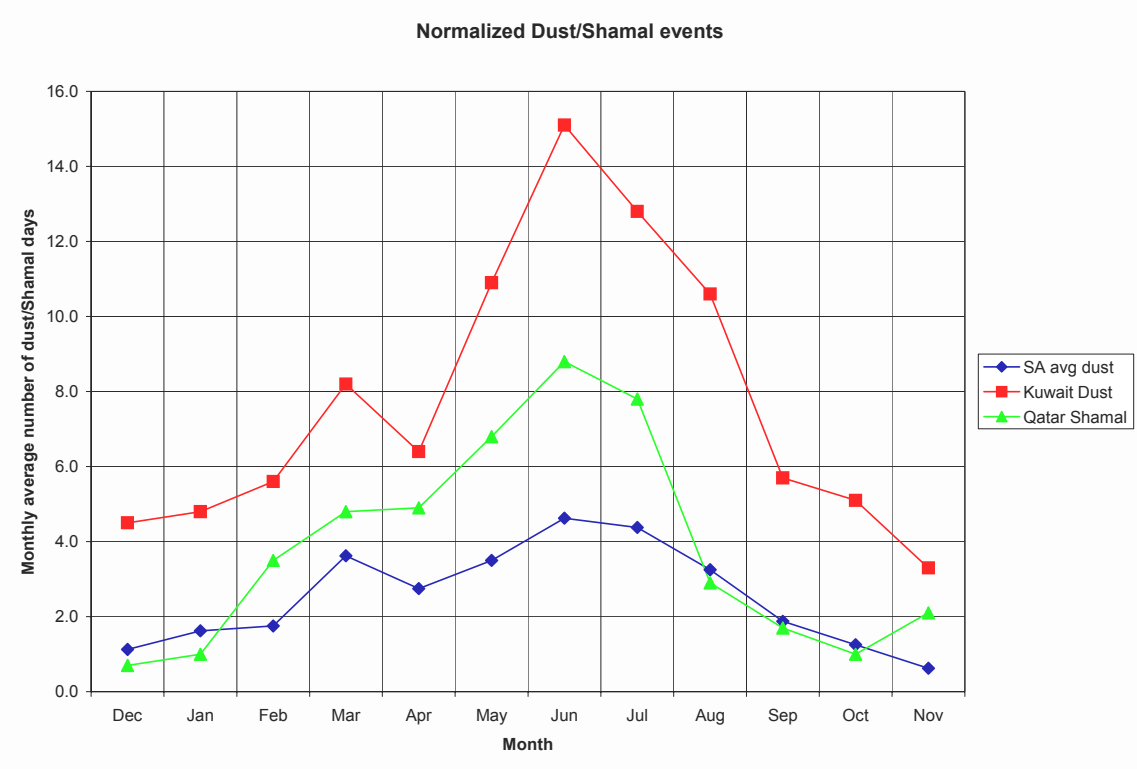

FIG. 11. Mean dust storm/Shamal occurrence for Saudi Arabia, Qatar and Kuwait. (Derived from Bukhari 1993, Rao, et al 2001 and Safar 1980).

Environmental Protection Administration data that consisted of satellite imagery and hourly surface observations from 8 Saudi Arabian weather stations over a 12 y period while studying dust events. In a similar study completed over 10 y at the Kuwaiti International Airport, Safar (1980) concluded that comparable spring and summer dust event peaks occurred within Kuwait. The most recent study completed by Rao et al. (2001), noted that over a 28 y period from 1962-1990 the Doha International Airport data also showed a similar seasonal distribution. Figure 11 shows that on average, Kuwait recorded the most dust storms within this region, followed by Qatar then Saudi Arabia. The number of reported storms and differences among the countries show a direct

correlation to each country's proximity to the primary dust source regions. The summer maximums common to each country depicted within Fig. 11 show that the dust storms are dependent on sparsely vegetated and dry soil source regions within Iraq and the AP, intense summer solar radiation and sustained surface winds common during the Summer Shamals. Finally, Fig. 11 provides the reader with a yearly outlook of trends and focuses the research on operationally significant seasonal dust storm events that affect Qatar.

III. Methodology

3.1 Overview

Greatly reduced surface based horizontal visibility is a crucial and measurable hazard affecting operations during dust storms. Developing a mesoscale forecasting tool that facilitates accurately forecasting these dust storms in Qatar is the main purpose of this study and involves five distinct processes. First, seasonal dust patterns are recognized through past data studies. Then, years of surface and upper air data from surrounding stations are collected and analyzed for climatological and dust advection patterns. Next, model output are archived from NAAPS, COAMPS and DTA models and compared with surface observations and MODIS satellite imagery to determine their ability to forecast and detect dust storm events. Then the dust data is grouped by location and the Al Udeid AB data is split evenly along seasonal lines and finally evaluated through CART decision trees and JMP derived multiple linear regression models to show how each parameter affected surface visibilities at Al Udeid AB, Qatar. The five step process is illustrated in the methodology flow chart depicted in Fig.12 and is described below.

First, seasonal and diurnal dust storm peaks and lulls are identified and understood by analyzing past regional studies. Figure 11 provides a graphical summary of the primary regional studies reviewed. Additionally the literature review reveals that sustained winds blowing at 10 m s^{-1} can lift sufficient dust into the air to reduce visibility in most cases and initiate a dust event. This correlates well with current dust forecasting

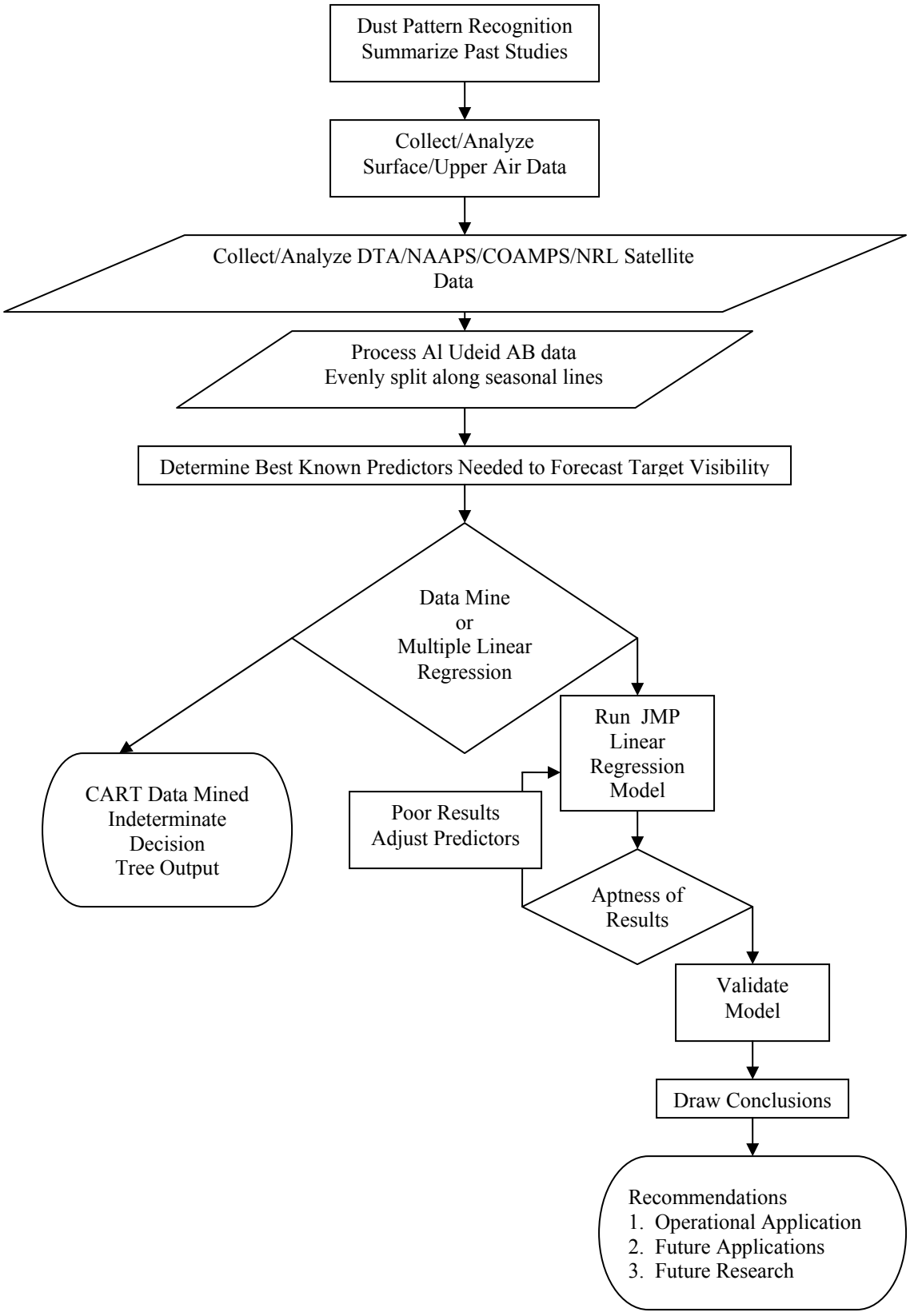

FIG. 12. Research Methodology flow chart.

guidance from the 28th OWS for weather stations in the region, which require a minimum sustained wind speed at 13 m s^{-1} to restrict visibility to 4800 m at most locations.

Once the seasonal peaks are identified, surface and upper air data are collected from surrounding reporting stations such as Al Jaber, Kuwait, Dhahran, Saudi Arabia, as well as Doha, and Al Udeid AB, Qatar encompassing data packages ten to thirty years long from the AFCCC. The collected data in comma delineated format is read into spreadsheets (e.g. EXCEL), where dust events are identified and analyzed for climatological and advection patterns.

Al Udeid AB operations have been limited to the past 2 y. Therefore once the seasonal and climatological patterns are established, the archived model output and satellite imagery for the past 2 y are evaluated to compare the model forecasts and surface observations and to provide additional relevant predictors for the subsequent regression analysis. Focusing on data collected throughout the whole year allows this study to evaluate the numerical and statistical model output through 2 y of known dust event peaks comprising the winter and summer seasons. As noted in the literature review, dust storms are the most intense in horizontal extent and duration during these two distinct winter and summer patterns and should be easily identified within the model output and enhanced satellite imagery collected.

The next step within the process is to pull the Al Udeid AB dust event data from the larger data pool, split the collected data evenly and statistically analyze the events. The Classification and Regression Tree (CART) software was originally used to identify relevant classification patterns, predictors and decision trees, but the results were difficult

to comprehend. Therefore the data is processed through JMP statistical analysis software to establish the best multiple linear regression analysis models. The resultant statistical analysis yields an "optimum" regression fit model that incorporates past studies of seasonal and diurnal patterns, model and satellite interactions as well as surface and upper air parameters and the accompanying synoptic weather patterns necessary to produce dust storms while accurately predicting the resultant reduction of visibility.

The closing process of this thesis is to summarize the statistical results and finalize a semi-automated forecast decision aid that is easily attainable and statistically proven against known dust events. The resulting decision aid will ultimately allow forecasters with limited regional weather knowledge to utilize the decision aid in conjunction with the AFWA and NRL products to easily identify and forecast mesoscale dust storm development at Al Udeid AB, Qatar in order to reduce the adverse effects of such weather phenomena on daily operations.

3.2 *Past Data*

To start, seasonal dust storm peaks and lulls are identified and understood by re-analyzing past regional studies that are discussed and summarized in detail within the literature review and Fig. 11. A brief summary of that chapter shows that there are distinct dust storm event peaks within the winter and summer of studied locations surrounding Qatar which are attributed to the transitory extra-tropical cyclones in the late winter/spring and the steady Shamal winds of a SSH. Dust storms are most intense in horizontal extent and duration during these two distinct seasonal patterns.

Additionally, past studies have shown that each studied site is sensitive to wind direction and the site's proximity to the major dust source regions. The current research exploits each reporting station's dependence on wind speed and direction to show the importance of the critical upper air and surface data in forecasting future events. Finally the literature review details valuable rules of thumb and forecasting techniques found in Table 2 that are instrumental in selecting initial predictors that can be used while forecasting visibility reductions through statistical linear regression techniques and are discussed in detail within the results section.

3.3 AFCCC Data

The author requested and received archived comma separated (CSV) surface observation and upper data from military and international reporting stations from the AFCCC worldwide database in Asheville, North Carolina. Surface weather observations are taken and transmitted worldwide every hour at the top of the hour. The military weather observations used within this study are also recorded and transmitted every hour. The surface parameters within hourly observations are recorded and transmitted as follows: time in UTC or Z, wind direction in degrees to the nearest 10˚, wind speed in whole knots, wind gusts in whole knots, visibility in meters, temperature in degrees ˚C to the nearest 0.1˚, dewpoint temperature in ˚C to the nearest 0.1˚ and altimeter in inches of mercury. Due to the expenses of maintaining, launching and recording upper air soundings, weather balloons are launched only twice a day at 1200 Z and 0000 Z from upper air sounding reporting stations around the world. The upper air parameters

measured are recorded as follows: time in Zulu (Z), atmospheric height measured in m, atmospheric pressure measured in mb, wind direction in degrees to the nearest 10˚, wind speed in m s^{-1}, temperature in ˚ C to the nearest 0.1˚, and dewpoint temperature in ˚ C the nearest 0.1˚. It is also prudent to note that every surface observation reporting station does not launch upper air sounding balloons. For purposes of research continuity, the surface and upper wind speeds are converted to m s^{-1} and maintained in scientific units throughout. Surface observations are normally available for review a few minutes past every hour whereas the upper air data may take up to an hour to be processed into useable form. Both data sources provide crucial information and are incorporated into the global meteorological models that guide the daily forecasts for cities worldwide.

The surface data collected are analyzed for stations surrounding Al Udeid AB such as Al Jaber, Kuwait; Dhahran, Saudi Arabia; Bahrain; Doha, Qatar, and Abu Dhabi, United Arab Emirates and can be found in Fig. 13. The data packages from surrounding stations span 10-30 y periods, however the data packages received for Al Udeid AB are limited to the period spanning March 2002 through September 2003 and reflect the short time that the base has been active. Due to the short data collection period for Al Udeid, climatological weather data has not yet been generated. The files of hourly observations from surrounding stations that encompass more than 10 y are large and cumbersome to analyze. Therefore each file is separated by station and blocks of years, but only data from 1990 to present are reviewed for this research project.

The surface observations are searched for reported dust in the present weather column at each station and highlighted accordingly. The highlighting process identifies a

significant amount of missing data within Special (off-hour) observations. Often the missing data can be extracted from the remarks section of the observation while retrieving data crucial to the research, therefore all of the observations are reviewed by hand to enhance the accuracy of the study and eliminate possible automation errors. The restrictions to visibility are then noted with dust events ≤ 4800 m highlighted and bolded. The highlighted observations from each of the surrounding reporting stations are then copied and transferred to another spreadsheet. Once the dust events are identified, the observations and satellite imagery are reviewed to see what environmental conditions existed before the onset of the dust event and possibly determine if the dust is caused by local, meso-scale conditions or by larger synoptic scale phenomena. Additionally, each weather observation preceding the marked events is scrutinized to determine additional factors such as how recently it had rained, how long it had rained and how many hours or days after the rain fell was dust able to develop.

Since the Al Udeid AB weather observations began in March 2002, the surrounding reporting stations are then broken into years, months, days and times that corresponded with the Al Udeid AB time frame. Then the surface stations are lined up within the spreadsheet as they fall along the Persian Gulf coast with Al Jaber, Kuwait first, followed by Dhahran, SA, then Al Udeid AB, Doha and finally Abu Dhabi as noted in Fig 13. This linear alignment allows a logical analysis of advected dust storms from Iraq and a quick view of how often dust is advected versus generated locally. Table 2 shows that the underlying physical processes are dramatically different for advected versus generated dust events. The northwest to southeast alignment, as well as how often the winds flow from a specific direction and how long they blow before dust onset also

provides valuable predictors of dust observed upstream later in the regression analysis and results sections. The final procedure for the surface observations at this point in the analysis is to copy and combine the Al Udeid AB observations for both years of the study into one large spreadsheet and readdress them later once all of the upper air, model and satellite data are input.

After the surface observations are scrutinized and dust events identified, the upper level data stations circled in Fig.13 are analyzed for possible patterns within the data. Geopotential height falls in the upper levels can sometimes signal the onset of advancing upper level cold air and potentially strong surface winds and are monitored around the time of each dust event. However, since the majority of the dust events climatologically occur during the spring and summer months it is noted that height falls are not common during most SSH events, but should be considered a significant predictor for winter Shamal events. Additionally, summer radiation inversions, winter frontal inversions and boundary layer winds within the upper air soundings are reviewed and considered preceding and during Qatari dust events to determine the factors affecting storm development and propagation. The outcomes are discussed within the analysis and results chapter.

The upper air data for the present study are analyzed from the nearest upper air sounding stations at Dhahran, King Fahad Airport, Saudi Arabia upstream and Doha Airport, Qatar downstream from Al Udeid and are encircled in Fig. 13. A temporal problem immediately develops when the upper air data are added to the daily observation worksheets. Upper air data is available every 12 h, yet surface observations are taken

every hour or sooner to note the sometimes rapid changes affecting surface parameters. Fortunately weather parameters measured above the boundary layer from launched weather balloons typically change less rapidly than at the surface. The upper air data is initially matched up with the corresponding times of surface data, then the upper air data is copied and matched with later surface observations until the next upper air data becomes available and the process is repeated until each dust event has surface and corresponding upper air data.

While collecting more recent data used in the analysis for Al Udeid AB there are many upper air data points that are missing between Dhahran and Doha. To rectify this, a

FIG. 13. Surface and upper level data source stations within SWA. The surface observation points are annotated by red dots with the upper level data points circled. (Adapted from 28th OWS CENTCOM website 2003)

statistical comparison between the two reporting stations approximately 128 km apart is completed. A sample of the statistical results seen in Fig. 14 shows that each comparative slope from the upper air data recorded between the geographically separated sounding stations approached 1. Therefore it is concluded that the upper air data from either station can be used interchangeably with little effect on the final model output. After the upper air data sets are combined as needed, the remaining few missing days of upper air data are filled with the FNMOC NOGAPS model output and manually input into the final spreadsheet. Once the upper air data is lined up by day and time, the upper air data is combined with the surface observation data in the final spreadsheet for further analysis with the model and satellite output.

3.4 DTA Data

The DTA model described earlier within the introduction uses a customized version of the Community Aerosol Research Model from Ames/NASA (CARMA) which ingests its upper level meteorological and surface terrain parameters from the AFWA MM5 output while incorporating dust source regions. In an independent study, Barnum et al. (2003) discovered that the DTA can successfully forecast synoptic scale dust storm occurrence and propagation in SWA the majority of the time, yet it cannot forecast meso-scale weather events well.

With these limitations in mind, DTA model output was requested and received from the AFWA/DNXT DTA model division encoded on a compact disk. The AFWA

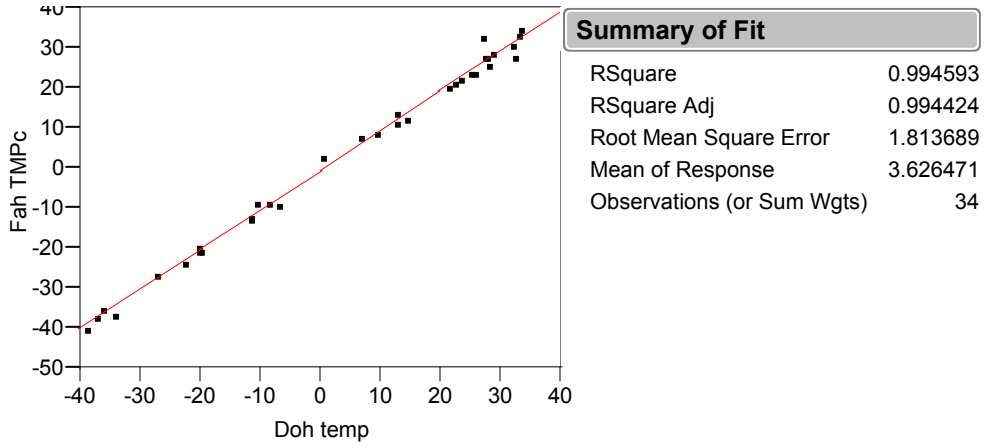

a. Temperature data.

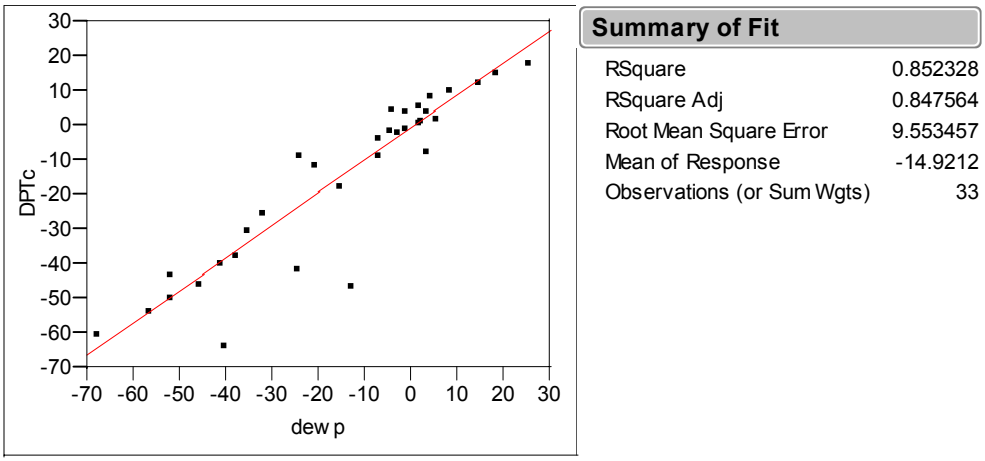

b. Dewpoint temperature data.

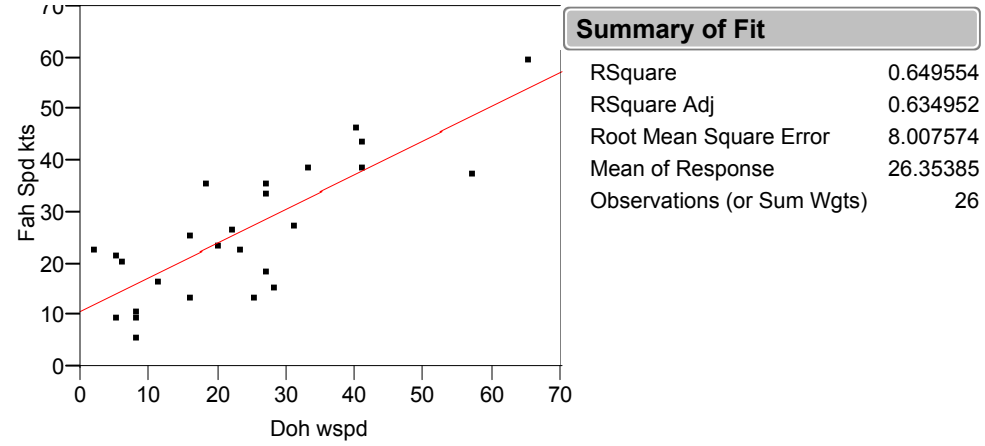

c. Upper air wind speed data.

Fig. 14. JMP statistical analysis comparing Doha and Dhahran upper air data.

provided daily model outputs that started at 0000Z and ended 72 h later at the 1800Z hour of the third day. The data was received in full color graphical form similar to what can be used any given day at the JAAWIN environmental website link. A typical output can be seen in Fig. 6 which encompasses the entire SWA region. The DTA graphical output is imported into a PowerPoint slide presentation and animated to show the dust storm forecasted progression and intensity.

DTA's color coded scale shows the model's forecasted dust transport concentrations at 100 m above the ground measured in $\mu g\ m^{-3}$. DTA tutorial guidance suggests that areas shaded yellow alert users in highlighted areas to the likely transport of dust with surface visibilities reduced to 4800 m, whereas areas shaded red alert forecasters to the likelihood of visibilities reduced to 1600 m (Barnum et al. 2003). The DTA model output is utilized as a first look as to when dust events affect Qatar within the current years peak dust season from March through September 2003. A dust event is identified by reviewing the first 4 images of the model, encompassing the first 12-h of the forecast on days of known dust events. Each day's model output is encoded within the master spreadsheet as "forecasted" or "missed" the dust event. The DTA model handles the majority of the synoptic scale dust events well; therefore the DTA is used as a predictor within the statistical model.

3.5 NAAPS Data

The NAAPS example model output found in Fig. 7 uses "a predictive, first

principle aerosol modeling approach wherein the sources and sinks are theoretically or empirically derived and depend upon the atmospheric fields forecasted by NOGAPS" (Liu et al. 2003). NAAPS acquires near real-time aerosol satellite data streams from AVHRR, TM/Landsat, TOMS and SAGE II polar orbiting and GOES satellites coupled with a global network of surface based aerosol monitors (AERONET). AERONET has 60 sun-sky monitoring spectral radiometers permanently deployed around the world including one at Bahrain. The data collected measure optical depth at eight wavelengths at one minute intervals and can be retrieved via satellite data streams (NRL 2003).

The NAAPS graphical plots found in Fig. 7 are available in two scales, global scale with the capability of 5-d outlook loops, and a user defined regional scale reduced to a 2-d outlook loop. These plots are best explained one panel at a time. The upper-left plot is the optical depth measured at a wavelength of 0.55 microns for three measured components: sulfate, dust and smoke. The sulfate contours start at 0.01 and double in magnitude for consecutive contours with the assigned colors varying from orange shades to red (NRL 2003). The upper-right plot is the sulfate mass mixing ratio measured in $\mu g\ m^{-3}$ at the surface. The contours start at 0.02 and double in magnitude for consecutive contours with the colors assigned the same as above (NRL 2003). The lower-left plot is the dust mass mixing ratio and is the plot that is monitored when forecasting dust in this region. The dust mass mixing ratio is measured in $\mu g\ m^{-3}$ at the surface. The dust contours begin at 20.0 and double in magnitude for consecutive contours with the assigned colors varying green shades through yellow (NRL 2003). The lower-right plot is the smoke mass mixing ratio measured in $\mu g\ m^{-3}$ at the surface. The contours begin at 0.2 and double in magnitude for consecutive contours with blue shades (NRL 2003).

The dust mass mixing ratio is the plot used for verification among the Al Udeid AB dust events highlighted earlier. A NAAPS dust column is added to the master spreadsheet and the archived NAAPS dust mass mix ratio outputs are reviewed for signs of dust during each event through September 2003. Because the environmental conditions inherent within this desert environment predispose the surrounding atmosphere with some level of dust year round, the NAAPS plots are closely scrutinized to determine what dust mass mixing ratio is necessary to reduce surface visibilities to 4800 m. A review of recent NAAPS plots, shows that shades of light green correlate well with reported dust at the surface reducing visibility to 4800 m. With the shade of green determined, the daily NAAPS plots are scrutinized on the dates of known dust events at Al Udeid and subsequent entries are made within the master spreadsheet as "forecasted" or "missed" the dust events. The NAAPS forecasts a majority of the synoptic events over the two-year period; therefore NAAPS is used as a predictor within the statistical model.

The NRL discussions of the NAAPS strengths include an integration of real weather into the model through NOGAPS, extended 120-h outlooks, operation in near-real-time, and global coverage with dust and smoke simulations (NRL 2003). The noted areas of work in progress for NAAPS include improvement of dust source functions, verification of the sulfate simulations and improved microphysics and chemistry. Some additional NAAPS operational challenges include but are not limited to determining the altitude of identified aerosols, identification and characterization of the source regions, conversion of synoptic observations to aerosol concentration and combining the data streams into a common format (NRL 2003). Despite the many challenges yet to be solved, the NRL continues to ingest data from multiple sources in countless spatial and

temporal scales and produce high quality aerosol guidance for the region. Because of the large scale of these challenges, the previously introduced NAAPS outputs remain in the developmental stage, are not always available and are not operationally tested and verified. However, when available the NAAPS outputs can provide a valuable tool for dust forecasting in Qatar.

3.6 COAMPS Data

The second NRL aerosol model is the latest version of COAMPS with an aerosol prediction capability released in March 2003. Similar to NAAPS the COAMPS aerosol model uses "a predictive, first principle aerosol modeling approach wherein the sources and sinks are theoretically or empirically derived and depend upon the atmospheric fields forecasted by COAMPS" (Liu et al. 2003). The COAMPS mesoscale aerosol model output shown in Fig. 8 is a recent addition to standard outputs that started development in 1977 when COAMPS was designed as a short term, 72 h meso-scale forecast tool for any region on the earth. Even though the current aerosol model output is not extensively field-tested, Liu et al. (2003) notes that a COAMPS 72 h forecast successfully covered the major dust event that crippled the AP from 25 – 27 March 2003 with wind and dust forecasts throughout the duration of the event. Since its recent inception, the aerosol COAMPS version is provided to field units for additional dust forecasting guidance only, though current research shows promise for COAMPS model output plots.

The COAMPS graphical plots as seen in Fig. 8 come in two grid resolution sizes, 81 km and 27 km, with the maximum capability of 72 h outlook loops at 3 h intervals

(NRL 2003). The graphical plots are best described one panel at a time. The upper-left plot represents the surface friction velocity patterns measured in cm s^{-1} in the form of blue stream lines with surface soil moisture measured in shades of green for dry to magenta for moist. The upper-right plot represents dust surface concentrations and is the plot of greatest interest when forecasting dust in this region, whereas COAMPS uses a threshold of 65 cm s^{-1} for dust lifting (NRL 2003). Initially the dust concentrations were measured in mg m^{-3} and coded in colors from blues for small concentrations to magenta for high concentrations of aerosols through the end of the 26 March 0000 Z model run. Figure 15 shows that starting March 27 at 0000Z, 2003 the dust concentration plots were changed to measure in μg m^{-3} to match standard mass mixing ratio measurement units while the color codes were shifted to 4 shades of color from blues for small concentrations to magenta for high concentrations. The lower-left plot is the dust optical depth coded in colors from blues to purples and has no units. The lower-right plot is similar to the NAAPS plot of the same position, but called the oil smoke mass loading measured in mg m^{-2} at the surface and coded in colors as above with blues representing minute smoke loads through purple for extreme smoke loads. The oil smoke loading plot was discontinued 26 April 2003 (NRL 2003).

Similarly to the quandary that arose while reviewing NAAPS plots, the environmental conditions inherent within a desert environment predispose the surrounding atmosphere with some level of dust year round. The COAMPS plots are closely scrutinized to determine the dust mass mixing ratio necessary to reduce surface visibilities to 4800 m. A review of recent COAMPS surface dust concentration plots

shows that shades of green are positive indicators of dust reported at the surface reducing visibility to < 4800 m. The upper-right plot of dust mass mixing ratio is the plot used for verification among the Al Udeid AB dust events highlighted earlier. A COAMPS dust column is added to the master spreadsheet and the archived COAMPS dust mass mix ratio outputs are reviewed for signs of dust as green shading during each event through September 2003 and noted within the spreadsheet. The COAMPS model forecasts a majority of the synoptic events over the two-year period; therefore COAMPS is used as a

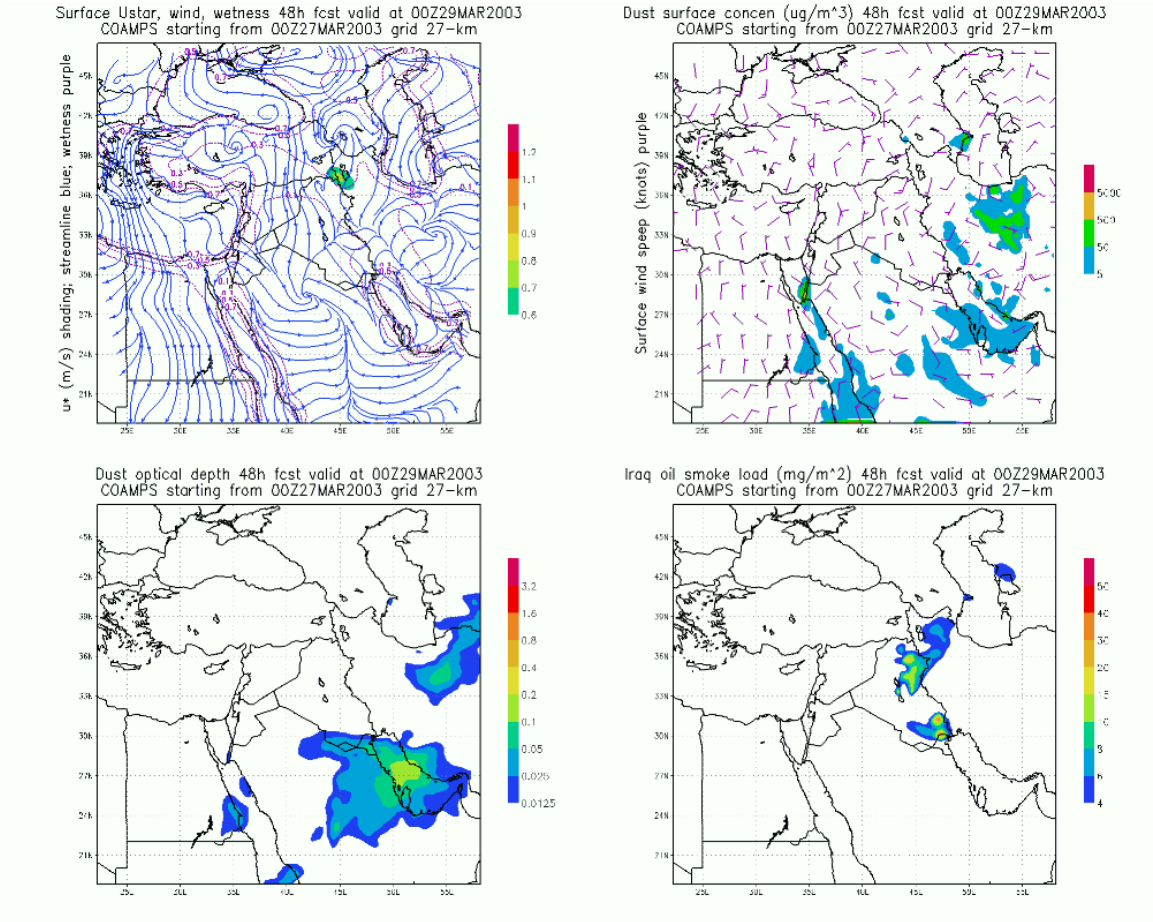

FIG. 15. Latest COAMPS dust concentration plot. Rescaled to μg m^{-3}. (Provided by NRL 2003)

predictor within the final statistical model. Because of the recent release of the COAMPS aerosol version, the previously discussed COAMPS plots remain in the developmental stage, are not always available and are not operationally tested and verified. However when available the COAMPS outputs can provide an additional tool for dust forecasting in Qatar.

3.7 Satellite Focus Data

The final NRL product used within the research to identify dust storm signatures is the "Satellite Focus" website which recently supplied and sustained deployed personnel with high quality satellite imagery. With the numerous successes of the "Satellite Focus" website, Dr. Miller and his staff have met the DoD task for the research community to become more "proactive" and "forward-focused" by pushing the technological envelope and fielding accessible, reliable and high quality satellite products that can directly enhance warfighter capability (Miller 2003).

A satellite dust column is added to the master spreadsheet and the archived satellite imagery outputs are reviewed for signs of dust during each event through September 2003 and noted within the spreadsheet. The enhanced archived satellite imagery detects a majority of the noted dust events over the two-year period; therefore the satellite imagery is used as a predictor within the final statistical model.

3.8 Data Splitting

With all of the past study knowledge, surface and upper air data, as well as model outputs and satellite imagery entered into the master spreadsheets, the data are split for regression analysis. Neter et al. (1990) notes that the best method to test and validate a regression analysis is to design the model with a test data set and validate the model by generating an independent validation data set. They also note that generating new data for validation is often not a valid option due to research limitations. Because generating a validation data set within the current research is feasible, the data sets within the master spreadsheets are separated into a test and validation data set.

There are many theories on how to best separate data when new data cannot be generated to test the validity of the regression model. Random divisions, 80/20, 60/40 and 50/50 data splits are all valid options, but for this investigation the database is split evenly. According to Neter et al. (1990), when seasonal data or cyclical events are being analyzed, such as seasonal dust storms, the data can be split as long as the remaining data sets are balanced. Therefore the data for this research is split and balanced such that dust events within each month or season are approximately equally represented within each data set. The new spreadsheets are renamed "test" and "validation" data set accordingly, and are put aside for further statistical analysis.

3.9 CART Data

As a test of its possible utility, a data mining technique using Classification and Regression Tree (CART) software is introduced to the research process. CART is designed to provide simplified decision trees based on specific statistical data splitting techniques that can evaluate thousands of multiple variables; categorize them into order of importance based on degree of changes in the data, and then split the data into branches of occurrence or non-occurrence at the point of CART defined most significant difference. CART continues the technique until the splits of data can no longer be completed due to lack of significant parameters to split (Salford Systems 1995). The CART process requires that data be pre-analyzed into classification categories of simple decisions. This allows the preliminary results to force a focus on the primary predictive targets that had been successful predictors in the past.

Using this technique, the CART program claims to simplify large sized, complex data patterns into easily identified general patterns of decision trees that help determine specific conditions necessary for identified event occurrence (Salford Systems 1995). Initially, CART requires multiple parameters of interest in order to prune the decision trees down to specific parameters of interest that isolate the current research target of reduced visibility. Unfortunately, within this research, CART produces very large preliminary decision trees with complex branches of parameter interaction that tend to split on seemingly random values within the predictor parameters. Because the initial CART decision trees are difficult to decipher with multiple splits of little physical

meaning, this study focuses on a multiple linear regression analysis to provide a more direct and interpretable solution.

3.10 Multiple Linear Regression

Many problems in the scientific community involve investigating relationships between two or more physical variables. These relationships can be analyzed through multiple linear regression techniques, but only after assumptions about the data population are made. For this research, data spanning almost two years from March 2002 through September 2003 are analyzed. Because the study focuses on dust events that reduced the surface visibility to $\leq$ 4800 m, the two year data base is reduced to 64 significant dust events, but among those 64 events there are 465 weather observations recorded. From the central limit theorem of statistics, a sample of data whose numbers or observations exceed 30 -- and are taken from a population that has an unknown probability distribution – is likely to result with a sample mean that is approximately normal (Montgomery and Runger 2003). Additionally the weather observations collected and used to develop the model are assumed to be independent of one another. The linear regression model's predictive parameters and resultant residuals are also assumed to be normally distributed random variables with common variance. Normality can be verified graphically by computing random scatter and normal plots of the residuals once the final model is derived, and is further discussed within the analysis and results chapter.

Multiple linear regression analysis is a statistical technique used to show the linear relationship between a response and multiple predictors and is chosen as the most effective statistical analysis for the current research. The research shows that as the number of predictors or weather parameters increases, the linear reaction with the response or predicted reduced surface visibilities becomes more intricate but can be solved through multiple linear regression techniques. The research goal of forecasting reduced surface visibilities can be described statistically with visibility measured in meters as the response variable or predictand, and the observed weather parameters and model inputs as the regressors or predictors. This can be represented by linear Eq. 1,

$$Y = \beta_0 + \beta_1 \cdot X_1 + ...\beta_n \cdot X_n + \varepsilon \quad (1)$$

where Y is the response variable, visibility; β_0 the intercept or "regression constant"; β_n "regression parameters", and X_n the variables or predictors with ε, residuals, assumed as the resulting random error with a mean of 0 and an unknown variance (Wilks, 1995). Wilks (1995) also notes that the residuals "correspond geometrically to the distance above or below this surface along a line perpendicular to the (X_1, X_2) plane." The positive multiple linear regression results achieved are relatively easily derived and understood. These results are also readily repeated through simple computer programs that can be forwarded to the end user. Therefore multiple linear regression is the statistical method chosen to best predict reduced surface visibility.

3.11 JMP Data

The aforementioned model and satellite imagery data are entered into the final

spreadsheets as valid predictors in the final linear regression model. The software used for the creation of the linear regression model is called "JMP". The JMP software package is designed by the SAS Institute as a "Statistical Discovery Software" widely used in advanced academic settings and industries worldwide. Once the surface and upper air data are effectively sorted within the spreadsheet and all parameters known to affect the surface visibility are included, the data is entered into JMP. Once opened in JMP, the final data files are scanned visually for occasional data points that are dropped when transferring from the spreadsheet software. In order to maximize the data points collected over the 2 y study period, dropped values are re-entered and saved. The JMP software allows a semi-seamless conversion from the spreadsheet software to efficiently evaluate dust event distributions such as maximums, minimums, means and trends of interaction between predictors and response parameters. In order to derive the dust storm distributions, a JMP "Fit Y by X" graphical option is invoked where the target variable of reduced visibility is compared with each surface observation parameter reported to determine the effect of each parameter on the visibility within all dust storm events. These data distributions are discussed in detail in the analysis and results chapter.

After the files are prepped, JMP is used to establish an "optimum" regression analysis to simplify the environmental predictors necessary to accurately forecast reductions in visibility and to determine specific conditions necessary for identified event occurrence. The most efficient way to achieve an "optimum" regression model is to use the Fit Model option.

Since the data population is seasonally split into separate test and validation data sets, the Fit Model is first applied to the test data set. The test data set is opened within

the Analyze Fit Model option as depicted in Fig. 16. The visibility parameter is entered as the Y or response variable the model tries to predict. The remaining parameters drawn from the columns of the test data set spreadsheet are then added to the model effects column or predictors as needed to fine tune the model.

The coefficient of determination (R^2) value is often used as a measure of the model adequacy in capturing the overall variability of the model. An R^2 of 1 would indicate a perfect model that predicted the response variable without variability. There is no limit to the number of predictors allowed within the fit model, however, in order to prevent over-fitting the test data set, the final predictors chosen are limited to field-accessible, meteorologically sound predictors such as satellite and dust model data, surface observations and upper air data. A Fit Model utilizing the primary predictors as seen in Fig.16 produces R^2 values climbing into the 0.70s. Including cross product interactions increases the response accuracy to R^2 values in the low 0.90s. To better understand multiple predictors and their interactions, the JMP derived R^2 adjusted statistic is also monitored. The R^2 adjusted statistic is a tool noted in Montgomery and Runger (2003) that lowers the R^2 value by the degree of over-fitting caused by too many predictors.

In addition to the R^2 values and the R^2 adjusted values, JMP standard Fit Model output shows Parameter Estimates which list each predictor and the statistical analysis of its performance within the model. Cross products whose Probability > t values exceed 0.20 are removed one at a time to improve both R^2 and RMSE values. This procedure is repeated until an "optimum model" is achieved. A final Forward Step Wise model run is then executed using 0.20 values as probability values to enter the model and 0.10 values

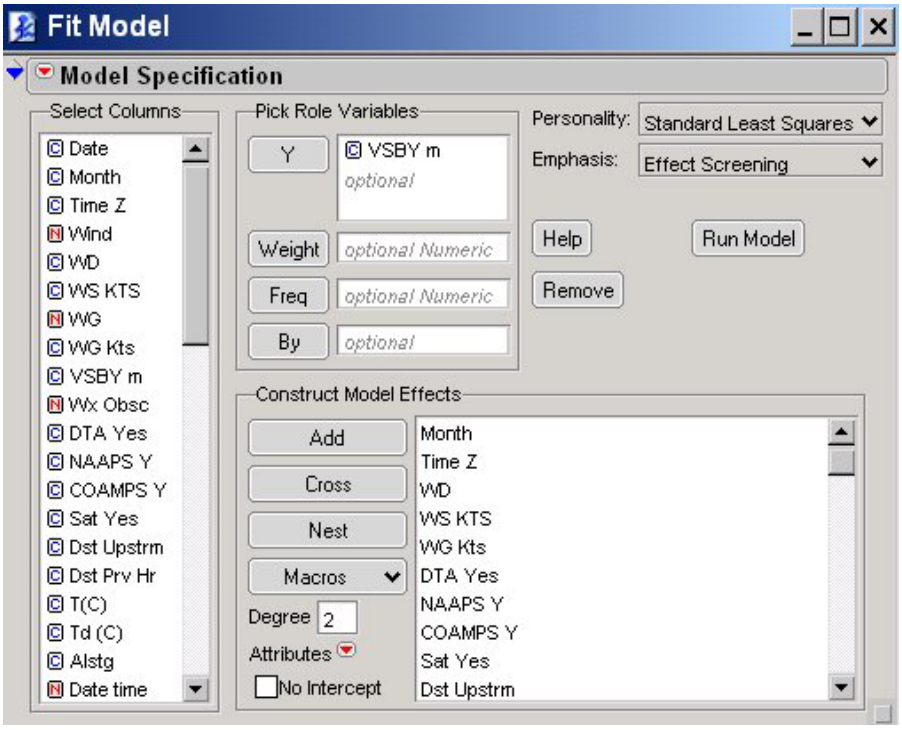

FIG. 16. JMP Fit Model interface. Used when creating standard least squares or stepwise models. (derived from JMP 2003)

to leave the model to eliminate predictor redundancies, simplify the model by cutting the total number of predictors from 90 to 53, and reinforce the validity of the initial model assumptions. With the R^2 value optimized for the test data set, the procedure is then applied to the validation data set with results discussed in the next chapter.

IV. Analysis and Results

4.1 Introduction

The previous chapter discussed the methodology used to sort, group, split equally along seasonal lines and analyze the data to develop an optimized fit model for the test data set that accurately forecasts the reduction of visibility due to dust-producing environmental conditions. The next 4 sections discuss the statistical analysis of significant dust events occurring during the study period, the optimized fit model developed with the test data set, the results of the fit model applied to the validation data set, and finally operational applications of the model.

4.2 Statistical Dust Event Analysis

An analysis of all the dust events affecting Al Udeid over the past 2 years reveals a spectrum of severity in dust storm phenomena. To quantify a physically meaningful dust storm threshold, a 3-step filter is applied to the events. First the study addresses the number of dust events occurring since Al Udeid AB began recording surface observations in March 2002 through the end of the study in September 2003. Secondly the research investigates the number of advected dust events that originate upstream compared to the number of dust events that are generated locally, and the different environmental conditions that foreshadow each type of event. Finally, the study addresses the monthly

occurrence, surface wind speed, gust, direction and resulting surface visibility statistical distributions during the significant dust events noted earlier.

Application of the 3-step filter noted above results in a significant dust event being defined as any observation where the visibility is reduced to ≤ 4800 m by any form of reportable dust. The current research is focused on the significant dust events because of the potentially adverse affects on flight operations. With these initial definitions in mind, Table 3 summarizes the yearly as well as total dust and significant dust events that occurred at Al Udeid AB.

The surface observations collected from AFCCC for Al Udeid AB, started in March 2002, so the annual dust events and significant dust events are tallied from March through December 2002, whereas the dust events for 2003 were counted from January through the end of the study in September 2003. The research found that observational data from early in 2002 was recorded approximately every 3 h during fair weather. Of the early 2002 surface observations reviewed, it appears that the observations were increased to hourly observations only when the predominant weather conditions adversely affected flight operations. Therefore the reliability of the observations collected within the first few months of 2002 are suspect and may show dust event anomalies when compared with data collected during the same period in 2003. The seasonal breakout of data is added as an additional row in Table 3 to capture the maximum number of dust events during the winter and summer Shamal events.

The resultant seasonal breakout as seen in Table 3 shows that the majority of dust and significant dust events occur during the Shamal seasons as discussed in the literature review. More pronounced seasonal differences are apparent between the 2 years as seen

TABLE 3. Summary of reported dust and significant dust events at Al Udeid AB.

		Dust Events	Significant Dust Events VSBY ≤ 4800 m
Year	2002	31	17
Season	Mar-Sep	24	**11**
Year	2003	95	47
Season	Mar-Sep	47	**43**
Year Totals	02 and 03	126	64
Season Totals	02 and 03	71	54

in Table 3. The dust season of March through September for 2002 yields 24 dust events that reduced visibility while the dust season for 2003 reports twice as many dust events with 47. The increase in seasonally significant dust events that reduce visibility ≤ 4800 m is more pronounced, as 11 significant events are reported from March through September in 2002, yet the same seasonal time frame in 2003 yields 43 significant dust events -- an approximate 4-fold increase. The reason for the noticeable increase is not inherently obvious from the data analysis, but a summary of possible solutions follows.

Limited observation reporting hours early in 2002 -- due to fewer military operations -- could be a source of some of the disparity in that some small-scale, between observation, dust events not reported in 2002 are reported in 2003. Additionally, the observation reporting procedures, such as day and night visibility marker locations could have been under development the first year and standardized the second year. Another possible source of the yearly difference could be increased anthropogenic activity in the form of Coalition ground troops who moved from Kuwait and into Iraq early in 2003. According to Clements et al. (1963) and Prospero et al. (1986), any increased anthropogenic activity across a source region surface greatly reduces the horizontal threshold velocity required to lift dust particles into the air. Therefore as tens of

thousands of Coalition troops in support of OIF drove across Kuwait and into southern Iraq during early spring of 2003, the desert source regions were likely disturbed, thereby providing additional dust sources. Another potential culprit for the yearly disparity could be increased farming along the fertile crescent of the Tigres and Euphrates river valley in southern Iraq due to the policy of the past government to drain the marshes in the region for agricultural use.

The literature review documented a higher wind threshold of 15 m s^{-1} for dust generation than for dust advection at 5 m s^{-1}. For this study a generated dust event is defined as an event that occurs locally at the reporting station and is not advected from a source region upstream based on wind direction. An advected dust event is defined as an event larger in horizontal and possibly vertical scale, reported upstream at most reporting stations, and transported downstream by strong surface and upper level winds. Additionally, dust events categorized by distant or local sources within this section are evaluated from the beginning of the study period in March 2002 through September 2003.

The data are separated and regrouped into advected dust events that originated upstream of Al Udeid or are generated locally. Once separated, the data show 103 surface observations capturing 21 significant dust events that are generated locally and 344 surface observations capturing 43 significant dust events that originate upstream and advect into Al Udeid AB. A brief discussion follows of some of the parameters monitored during significant dust events that reduced visibility ≤ 4800 m. at Al Udeid AB. These parameters are summarized in Table 4.

The most striking difference among the two events is the apparent dominance of the advected events, as there are twice as many advected dust events, and three times as many recorded observations during those events. Additionally the advected events sustain poor visibilities for up to 2.5 d whereas the local events are limited to 10 h. Thunderstorms also contribute to the higher number of advection events with 9 additional reports.

Outside the dominance of the advected events, the remaining differences shown in Table 4 are more subtle. The mean month and time of occurrence, surface wind direction, as well as speed and gust are strikingly similar considering the differences in number and duration of events. Some atmospheric differences become more apparent

TABLE 4. Local and Advected dust event summarization.

	Local	Median	Mean	Advected	Median	Mean
Surface Observations	103			344		
Significant Dust Events	21			43		
Minimum Duration h	1			1		
Max Duration h	10			24		
Max Duration d	0			2.5		
Duration h		3	3.7		5	6.3
Thunderstorm associated	2			11		
Visibility m		3200	3347		3200	3067
Month		5	5.6		5	5
Time Z		10:00	9:49		10:00	10:51
Surface Wind Direction		330	250		320	256
Surface Wind Speed m s^{-1}		7.2	7.6		7.2	7.5
Surface Wind Gust m s^{-1}		13.6	13.3		13.9	13.6
925 mb Temp C		26.2	27		31.8	29
925 mb Wind Speed m s^{-1}		10.3	9.6		10.3	10.5
925 mb Wind Direction		290	226		305	267
850 mb Temp C		23.2	23.2		25.8	24
850 mb Wind Speed m s^{-1}		5.2	7.6		11.3	11.4
850 mb Wind Direction		265	257		300	283
500 mb Heights m		5836	5811		5846	5832

within the first couple of mandatory upper level layers. For example, a 2˚ C increase in the mean 925 mb temperature during advected dust events could be a reflection of a surface based temperature inversion that restricts surface mixing while maintaining suspended dust near the surface with reduced visibilities. The inversion may also hold the 1 m s^{-1} stronger mean winds aloft to continually transport the dust further downstream through extended dust fallout. The 925 and 850 mb wind directions for local events show a southwestern trend compared to the more westerly to northwesterly directions of the advected events. The northwesterly wind direction at the 925 and 850 mb upper levels was a positive precursor to advected events during the summer dust study at Dhahran AB, Saudi Arabia (AFCCC 1957). Finally, the strongest difference apparent at the upper levels is the 850 mb wind speed where the advected events show a mean increase of 3.8 m s^{-1} over the local events. Notably, the AFCCC (1957) dust study claims that wind direction aloft is the main contributor to the advected dust events and that wind speed is "of little consequence." However the Dhahran dust study was focused on SSH events, whereas the current research at Al Udeid AB encompasses yearly dust events, so the discrepancies noted can possibly be explained by the seasonal restrictions of the Dhahran study.

Overall, the atmospheric contrasts between locally generated and advection dust events are subtle and offer little guidance to discern between forecasting local versus advection events. However, the main points that can be gathered from the dust storm summary are that advected events occur twice as often, last twice as long, are more common with stronger northwesterly winds aloft and surface wind gusts whereas local

events are more likely to be generated with a southwest to westerly surface component to stir up surrounding local dust sources for a much shorter period of time.

Finally, a JMP statistical dust event analysis is conducted to address the monthly, surface wind speed, gust, direction, upper air wind speed, direction and resultant visibility distributions encapsulating all of the local and advected dust events. A brief description of each parameter's distribution follows.

The first distribution of significant dust event parameters analyzed using JMP are the months of occurrence and can be found in Fig. 17. This bar chart shows a trend similar to the event distributions seen in Fig. 11 and discussed in Table 4 where March shows a marked increase with a secondary peak into May. The monthly bar chart within Fig. 17 is skewed by the number of observations taken in May during an extreme 2.5 d SSH event; otherwise the distribution follows seasonal patterns apparent in Fig. 11 as expected.

Figure 18 shows the wind direction distribution during significant dust events and

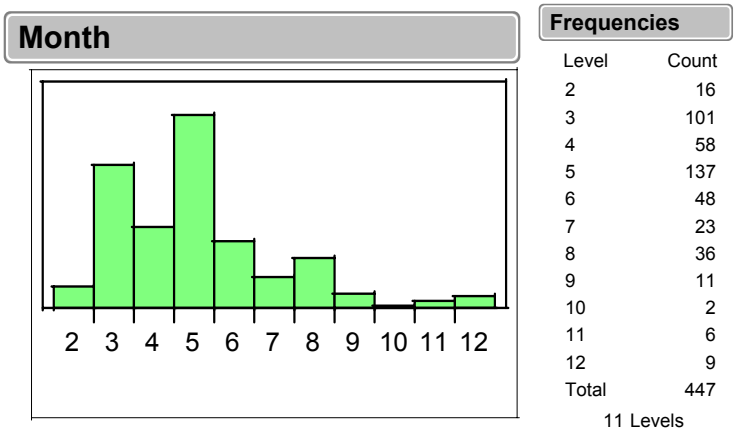

FIG. 17. JMP monthly distribution of surface observations taken during significant dust events for 2002 and 2003.

shows the median or mid point of all recorded wind directions is 320˚ with the mean of 271˚. This wind direction is consistent with the northwest annual mean wind directions recorded throughout the region.

The third distribution of observed dust event parameters analyzed is wind speed as shown in Fig. 19. The wind speed distribution shows that during the significant dust events recorded, the maximum sustained wind speed is 17.99 m s^{-1} with the minimum recorded as calm winds. The median or mid point of dust event wind speeds is 7.2 m s^{-1} with the mean at 7.5 m s^{-1}. This mean wind speed is consistent with winds required to advect dust defined earlier as 5 m s^{-1} and stronger than the climatological wind speeds recorded at nearby Doha International Airport that shows an annual mean wind speed of 5.7 m s^{-1} (AFCCC 2003).

The fourth distribution of dust event parameters analyzed is wind gusts as shown in Fig. 20. The wind gust distribution shows that wind gusts were recorded at only 323 of the 447 significant dust event observations. The reduced number of recorded gusts

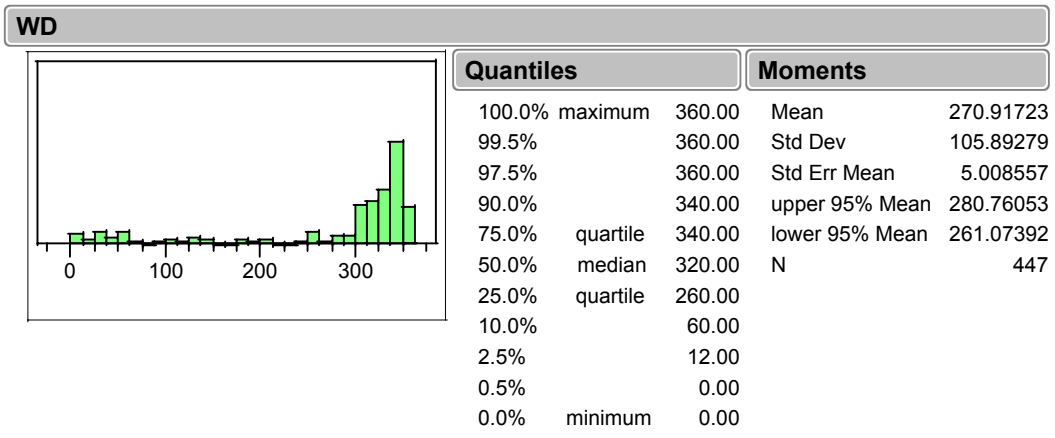

FIG. 18. JMP wind direction distribution of surface observations taken during significant dust events for 2002 and 2003.

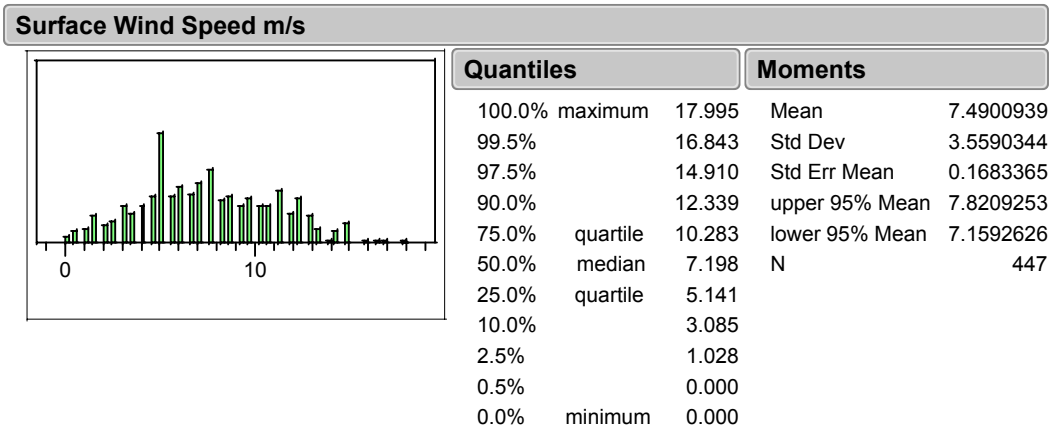

FIG. 19. JMP wind speed distribution of surface observations taken during significant dust events for 2002 and 2003.

indicates the sporadic nature of wind gusts. The maximum wind gust shown is 23.65 m s^{-1} with a minimum gust recorded at 6.2 m s^{-1}. The median or mid point of recorded wind gusts is 13.88 m s^{-1} with the mean at 13.6 m s^{-1}. Wind gusts are described within the literature review as a necessary forcing mechanism to lift the dust into the air as well as turbulently mix the dust near the surface.

The final distribution of dust event parameters analyzed, the surface visibility

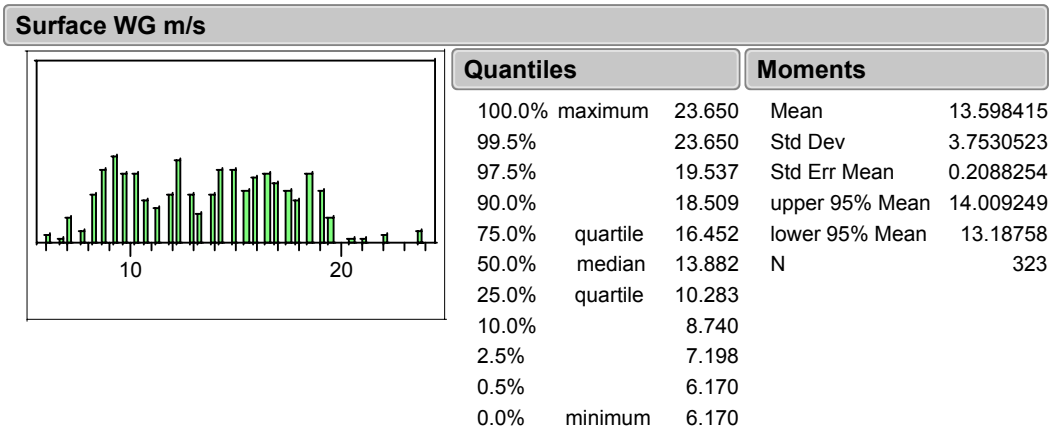

FIG. 20. JMP wind gust distribution of surface observations taken during significant dust events for 2002 and 2003.

distribution is the primary focus of this investigation and is illustrated in Fig. 21. The visibility distribution shows that during significant dust events, the maximum visibility is at 4800 m with the minimum reduced to 200 m. The median or mid point of dust event visibilities is 3200 m with the mean of 3127.5 m. The mean visibility of 3127.5 m is a direct result of the mean wind direction from the west at 271˚ coupled with the mean wind speed of 7.49 m s^{-1}. The mean wind direction and wind speed are also consistent with wind directions and speeds required to advect dust defined earlier as northwesterly wind directions and wind speeds of at least 5 m s^{-1}.

Both the mean direction and wind speed results are slightly different from past guidance. The literature review noted that most reporting stations in the AP region require a more northwesterly flow and stronger winds closer to 13 m s^{-1} to reduce visibility. Additionally the mean wind speed at 7.49 m s^{-1} is lower than past forecast guidance from the 28 OWS (2003) that sets a 13 m s^{-1} threshold to reduce visibility to 4800 m. Hence the differences inferred from this study suggest that the increased activity

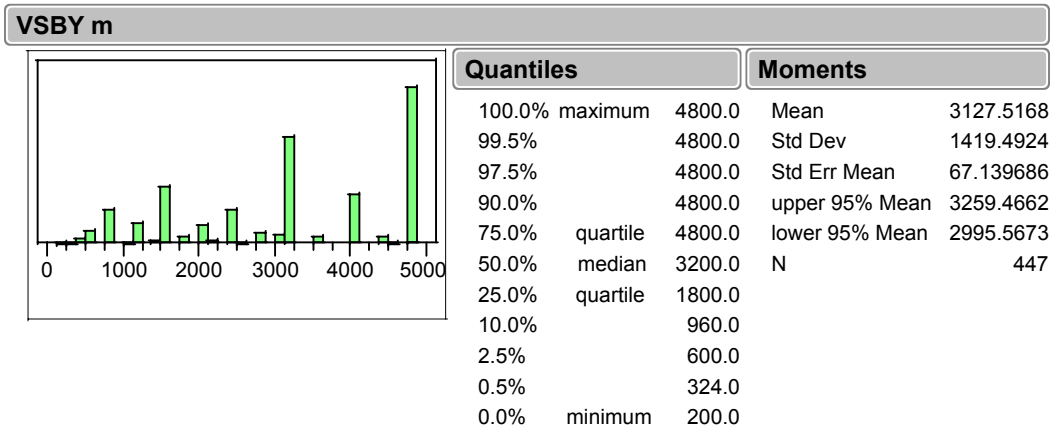

FIG. 21. JMP visibility distribution of surface observations taken during significant dust events for 2002 and 2003.

at Al Udeid AB over the past two years has both enhanced dust suspension and improved dust reporting.

The dust storm distribution and analysis of key parameters discussed previously show the importance of many of the key surface predictors and their roles in visibility reduction. The primary predictors that are used to finalize the model are chosen with consideration of past studies, trial and error tests within the model, and their availability to the operational forecaster. These predictors are listed below in order of model appearance: month, time, surface wind direction (WD), surface wind speed (WS), surface wind gust (WG), surface altimeter, DTA forecasted dust, NAAPS forecasted dust, COAMPS forecasted dust, satellite imagery depicted dust, dust reported upstream, surface temperature (T), surface dewpoint temp (Td), 925 mb T, Td, WS, WD, 850 mb T, Td, WS, WD, 500 mb T, Td, WD, 300 mb T, Td, WS and WD. The remaining predictors used are derived from cross products of the primary predictors and are listed in Table 7 in the Appendix.

According to Wilks (1995), transformations of predictors, such as cross products, can sometimes lead to a better understanding of the physical processes behind the phenomena being studied. However, Wilks (1995) also notes, that if a better forecast about the phenomena being studied is the ultimate goal, then the physical processes involved are sometimes less important than the final outcome. Because the current research is focused on the forecasted reduction in visibility, a full explanation of the complex physical interactions is considered unnecessary. Therefore no effort is made to explain why the 25 cross products introduced within the research increase the validity of the best Fit Model derived.

4.3 Test Data Results

Based on the statistical results of the significant dust storms and the discussions of the predictors within the previous two sections, a multiple parameter linear regression Fit Model from the JMP software is obtained using 28 primary predictors coupled with 25 cross product derived predictors shown in Table 7 of the Appendix. This section first addresses the JMP Summary of Fit results that include R^2, R^2 adjusted, RMSE, the mean of the response, a 95% prediction interval, then it discusses the overall F-test results and finally it discusses the resultant residual plots and how they relate to the validation phase of the model.

The Summary of Fit statistical results from the "optimum" Fit Model are shown in Table 5. The R^2 value of 0.91 is a highly regarded model output because this implies this model's ability to capture 91% of the variance of the outcomes. The R^2 adjusted of 0.87 is also desirable since an R^2 adjusted statistic near the R^2 value indicates the regression is not over-fit with excessive predictors. The Root Mean Square Error (RMSE) of 514 m is also encouraging and perhaps the most impressive result as it suggests the model could provide an operational forecaster a visibility prediction tool accurate to within 1/3 of a mile.

Given that the RMSE meets the research objective of "accurate to within 800 m," the regression fit model is considered optimized. Thus adjustments are halted with a final test data set Mean of the Response of 2953 m. Mean of the Response or the predicted visibility is the mean of the best fit model predicted visibility in meters which is used to compute a 95 % prediction interval. The test data set computed prediction interval or

TABLE 5. JMP derived test data model statistical output.

Test Data set Summary of Fit	
R Squared	0.9149
R Squared Adj.	0.8684
Root Mean Square Error	514.43
Mean of Response	2943.05
Observations	151
Prob > F	< 0.0001
Mean Square Error (MSE)	264,640

probability of predicted values falling within that 95% prediction interval is later used to further determine the adequacy of the best fit model when applied to the validation data. The observations value is simply the number of surface observations from the test data set that the model uses while deriving the statistical model output.

The final statistical value computed within Table 5 is the Prob > F which is the overall F- test or the statistical probability of "obtaining a greater F-value by chance alone if the model fits no better than the response mean" (SAS Institute 2003). Since probabilities of $F < 0.05$ show that there is significant regression within the model being fit, the Prob > $F < 0.0001$ value that is derived while fitting the current model offers further proof that the best Fit Model depicts significant regression and is a model worth investigating further with additional tests.

The final statistical test to determine the adequacy and reliability of the fit model developed is to review the Residual plots found in Figs. 22 and 23 to assess the randomness, heteroscedasticity or non-constant variance and normality of their plotted patterns (Wilks 1995). Residuals, as discussed earlier, are the difference between the observed and predicted visibilities. Therefore when the Residuals yield an objectively random scatter pattern as seen in Fig. 22 and an approximate normal distribution as

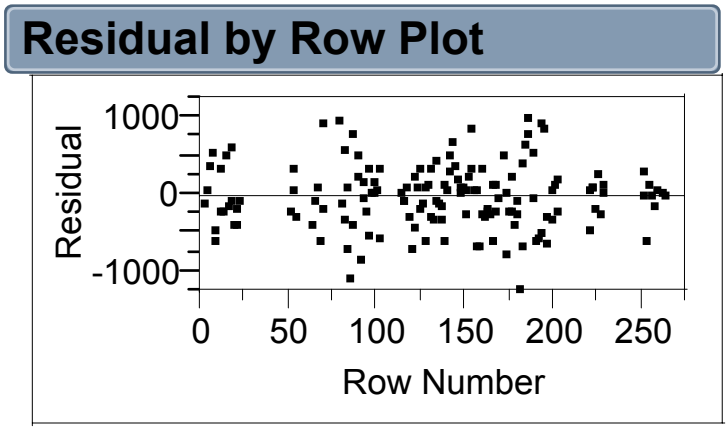

FIG. 22. JMP derived test data set model residual plots by row.

shown in Fig. 23, then the fit model results can be considered legitimate. Therefore due to the high valued R^2, and R^2 adjusted values near 0.90, the RMSE < 800 m, the Prob >F < 0.0001, the randomness of the residual plot, and finally the normally distributed residuals, the fit model is deemed optimized and adequate for application to the validation data set.

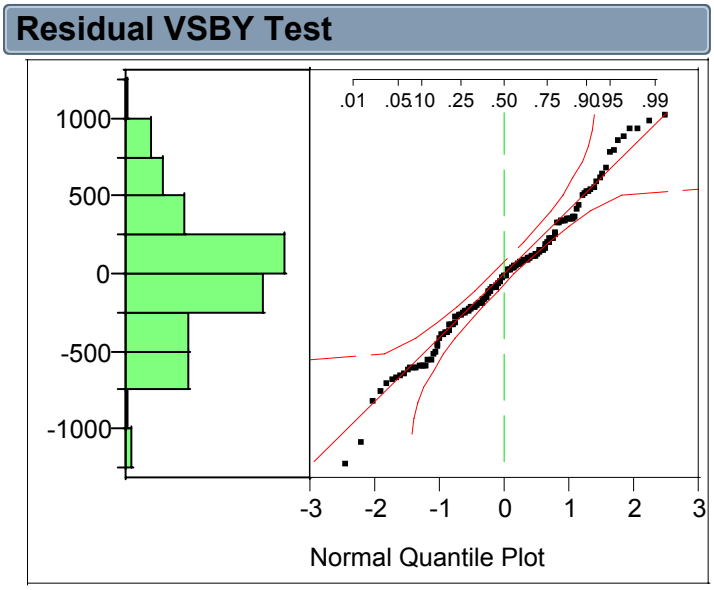

FIG. 23. JMP derived test data set normal plot of residuals.

4.4 Validation Data Set Results

For this study, the model's ultimate validity is tested by running the same predictors derived from the test data set and applying them to the previously separated and held-back validation data set. The Fit Model option is run again within the JMP software using the 28 primary predictors listed within the previous section coupled with 25 cross product predictors that can be found in their entirety within Table 8 of the Appendix. The analysis of the model validation found below follows the same process described in the test data discussions.

Table 6 contains the Summary of Fit statistical results for the validation model. The R^2 value of 0.79 from the validation data set is considered an acceptable model output -- despite the drop from 0.91 for the test data set -- because the coefficient of variance or R^2 describes this model's ability to capture 79% of the variance of the predicted responses. The R^2 adjusted of 0.66 is also considered valid as it is close enough to the R^2 value to demonstrate that the model is not over-fit. The RMSE of 740 m shows an increase from the test data RMSE of 514 m but still remains below the desired accuracy of < 800 m. The Observations value of 137 shows a slight decrease from the test data due to additional missing data points within the validation data set. The Mean of the Response at 3368 m indicates that 63% of the validation data set predicted visibilities fall into the 95% test data set prediction interval and further attests to the best fit model's validity.

The Prob > F value for the validation data set is similar to the value for the test data. Since probabilities < 0.05 show that there is significant regression within the model

TABLE 6. JMP derived validation data model statistical output.

Validation Data set Summary of Fit	
R Squared	0.7944
R Squared Adj.	0.6631
Root Mean Square Error	739.72
Mean of Response	3367.88
Observations	137
Prob > F	< 0.0001

being fit, the Prob > F < 0.0001 value found offers further proof that the model results are reasonable and significant. As a further test of the output validity, the residual random scatter and normality plots are examined. Figure 24 illustrates the rather random scatter of the validation data set residuals. Figure 25 depicts the nearly Gaussian nature of validation residual distribution. Both of these results further exemplify the suitability of the model output.

The final means to measure the aptness of the regression model derived is to measure the predictive capability of the model (Neter 1990). Using the residuals from the validation model output along with the number of observations taken into consideration, a Mean Square Prediction Error (MSPR) is computed using Eq. 2 and is explained in greater detail below,

$$\mathrm{MSPR} = \frac{\sum_{i=1}^{n} \left(Y_i - Yt_i\right)^2}{n} \qquad (2)$$

where *Yi* is the value of the response variable in the *ith* validation case, *Yti* the predicted value for the *ith* validation case using the derived model from the test data set and *n* the number of observations within the validation data set (Neter 1990). The MSPR checks

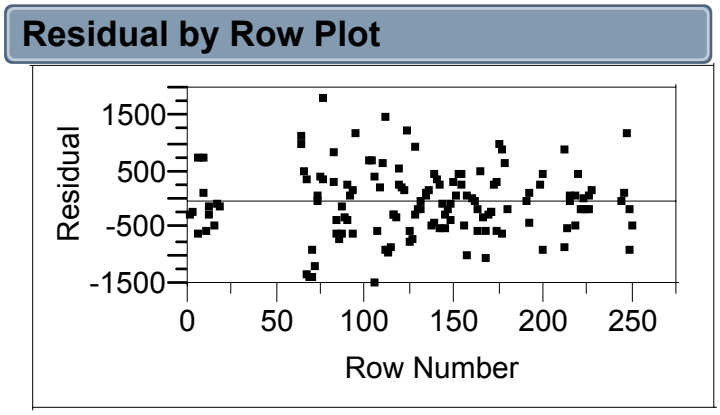

FIG. 24. JMP derived validation data model residual plots by row.

the predictive capability of the validation model by comparing the MSPR computed value to the Mean Square Error (MSE) from the "model building" test data set (Neter 1990). When the two values are relatively close, this is a good indicator of the model's aptness, the derived model is considered non-biased and shows the model's predictive abilities (Neter 1990). Since the MSPR computed at 362,917 is well within an order of magnitude of the model building MSE of 264,640 from table 5, the optimized fit model is considered non-biased with a positive predictive capability.

In summary, the optimized model is considered a suitable statistical model due to the closeness of the R^2, and the R^2 adjusted values, the RMSE < 800 m, the overall F-test with a Prob >F < 0.0001, the randomly scattered and normally distributed residual plots, the prediction interval that captured 63% of the validation data, and the closeness of the MSPR and MSE. Thus the optimized Fit Model can be applied to Al Udeid AB meteorological scenarios with confidence that it can predict reduced visibilities accurately.

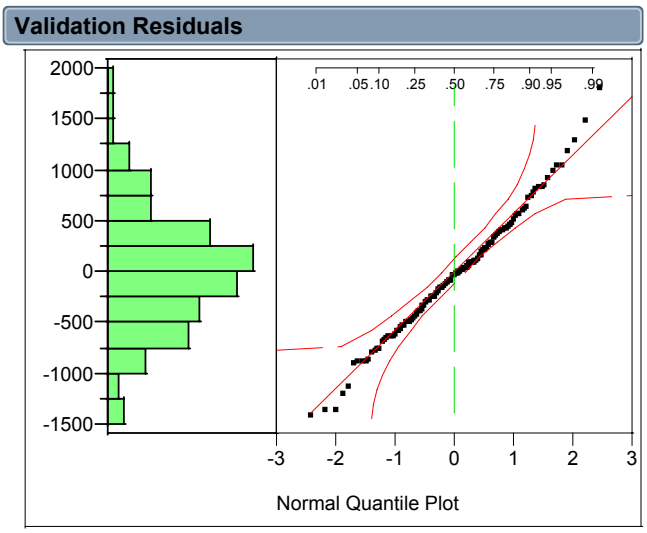

FIG. 25. JMP derived validation data set normal plot of the residuals.

4.5 The Optimized Dust Prediction Application Model

With the statistical model derived, the results analyzed, and the model accepted as predicting response values accurately within the population of data, the research now focuses on creating a simple and semi-automated application of the resultant linear regression equation. This regression equation could be loaded into an EXCEL or EXCEL-like spreadsheet and forwarded to the end user. The AUDust (for Al Udeid AB Dust) spreadsheet simply uses the linear equation parameters and estimated values calculated within the optimized Fit Model derivation found in Table 8 (see Appendix) to transform the automated statistical JMP output into a field accessible spreadsheet for future applications.

The resultant AUDust spreadsheet requires the end user to enter 28 surface based and upper air forecasted values into the spreadsheet where the linear algorithms then

calculate the predicted surface visibility. The 28 parameters may seem like a large number of manual entries, but most parameters can easily be drawn from standard mesoscale model outputs and require only a few numerical key strokes. It should also be noted that no values within the primary 28 key parameters can be skipped or missing. Each predictor has sufficient weight within the optimized model such that if one key predictor is missing no forecast can be made. It is further noted that if no wind gust is available, the surface wind speed can be substituted with little adverse affect on the final outcome. Again the fact that all 28 predictor parameters are routinely available via standard mesoscale model output prevents the "no missing data" requirement from being prohibitive.

The operational significance of the summary of seasonal and type of dust storm distributions, meteorological parameters and resultant "optimum" Fit Model are apparent. The seasonal patterns and dust storm type summary offer operators within the region a synopsis of possible dust prone periods and duration of events; whereas the "optimum" Fit Model offers an accurate dust forecasting tool. Furthermore, the "optimum" Fit Model developed within this study incorporates recent Air Force, Navy and NOAA products with easily attainable surface and upper air data into one well-balanced statistical model that accurately forecasts reductions in visibility to < 800 m.

V. Conclusions and Recommendations for Future Research

5.1 Conclusions

The primary goal of this research is to provide the 28th OWS weather forecasters a simplified tool to help forecast mesoscale dust events at Al Udeid AB, Qatar. This goal is achieved through an extensive statistical analysis of observational data depicting significant dust events over the past 2 y. The resultant statistical model derives and combines 28 easily attainable surface and upper air observations, model outputs, satellite images, and applies a linear transformation equation while providing the end user with a numerical visibility forecast for Al Udeid AB accurate within 800 m. Additionally the developed forecast tool provides the end user with a proven statistical model that is verified against a seasonally divided and independent validation data set that yields an R^2 of 0.79, an R^2 adjusted of 0.66, an RMSE < 800 m, an overall F-test with a Prob >F < 0.0001, as well as randomly scattered and normally distributed residual plots. Fielded combat weather teams are expected to be better prepared to support the ever changing flying missions operating within the region as a result of this investigation.

This research additionally demonstrates a method to statistically analyze the significant dust events and show the distribution of key visibility reducing dust predictors such as time of year, wind direction, and wind speed at the surface and aloft. The derived distributions show the dependence of the dust events on these key parameters and the many triggers needed to create a significant dust event that reduces surface visibilities

and affects daily operations. One main point the dust storm distributions reveal is the mean wind speed at 7.49 m s^{-1} is lower than current forecast guidance from the 28 OWS (2003) that states a 13 m s^{-1} threshold to reduce visibility to 4800 m. This difference suggests that the increased activity at Al Udeid AB over the past two years has both enhanced dust suspension and improved dust reporting.

A further benefit of this study is that it confirms that recent dust satellite enhancement and dust forecasting model advancements can be linked and applied to dust events within this region. Close contact with the AFWA, the NRL Aerosol modeling agencies, as well as, the NRL Marine Meteorology and Satellite Division, led to the linkages discovered. There have been great strides made towards research, development, and field-testing of the new aerosol models and satellite enhancement techniques within the past two years. These rapid advancements have also been made due to the concentrated efforts of the research community to understand the time sensitive nature of an operationally driven need for better forecasting products. Drawing from the strengths of recent research developments from each individual agency, the statistical model developed herein incorporates products from the AFWA and NRL divisions into the final mesoscale forecasting tool. Yet despite all of the advancements made, limitations still remain.

All three aerosol models noted above rely heavily on space-based, remote sensing of micro to synoptic-scale dust source regions and are thus limited to the sometimes coarse resolution of the remote sensor. Resolution limitations force assumptions to be made about soil composition and complexity. The assumptions about the earth's surface

coupled with the standard atmospheric modeling assumptions inherent within each model lead to unavoidable errors in model output. The "optimum" Fit Model developed weighs the inherent errors equally as it combines all models, with satellite output, ground truth and upper air sounding data to develop a linear model that successfully predicts the visibility at a mesoscale level. With that in mind, the resulting linear algorithm is now dependent on additional forecasted data to create the point forecast at Al Udeid AB. Therefore the resulting statistical visibility forecast is limited by the ability of the aerosol models and forecaster experience to predict the nature of the atmosphere at Al Udeid AB.

5.2 Recommendations

5.2.1 Recommendations to AFWA. The statistical model developed from the past 2 y of model outputs, satellite imagery and observed surface and upper air data requires an accurate model input to forecast the surface visibility. It is recommended that the AFWA incorporate the current dust specific "optimum" Fit Model into a MOS type output using the "model of the day" data as input. Then the model driven forecast can be provided to the end users at the 28th OWS where they can determine the true feasibility of the statistical tool.

5.2.2 Recommendations for further research. Although this research provides useful results and an extended dust/sand storm forecasting technique, there is room for

improvement on the processes. The entire process should be verified operationally with ground, and air truth observations as well as pilot reports (pireps) for an extended period of time and adjusted accordingly. It is also recommended that this statistical process be applied to additional locations in the region to determine the feasibility of model usage at other operational sites within the AOR.

The linear regression technique demonstrated herein could possibly be further improved using a Neural Net non-linear regression approach. The JMP Neural Net modeling technique is based on a nonlinear regression model that fits the model through "standard nonlinear least-squares regression methods" (SAS Institute 2003). An advantage of a Neural Net model is that it can "efficiently and flexibly" model multiple response surfaces through the introduction of hidden nodes (SAS Institute 2003). The JMP tutorials from SAS Institute (2003) note that Neural Net models are normally fit to held back data or test data sets similar to the linear regression processes and validated on the remaining validation data set.

Some of the disadvantages of the Neural Net are that the results are not easily interpreted, Hidden Nodes tend to obscure the processes, the models very easily over-fit the data and the fit is not always stable. Also, the Neural Net estimates the model from different starting points along a non-linear S shaped curve from randomly selected starting points and yields different statistical results every time it is run, which may not be the optimal answer (SAS Institute 2003). In light of the advantages and disadvantages described, the Neural Net is considered as worthy of further investigation. For comparison, when the original 28 primary predictors of this investigation are inputted

into a JMP default Neural Net model and applied to the validation data set, the program yields an impressive R^2 of 0.93. Due to time limitations, these Neural Net results are not pursued any further, but are believed to warrant further research.

Since the current research goal is to develop a forecast tool that helps weather forecasters predict reduced visibility due to dust, the research evaluates all reported dust events -- both suspended and blowing dust events. The atmospheric properties driving both conditions are vastly different, yet related. It is recommended that as additional years of surface and upper air data become available at Al Udeid AB, the problems of forecasting suspended dust compared to blowing dust be reevaluated as a separate topic. It is believed that the results may deviate from the current research and could shed additional light on the dust forecasting challenges.

Glossary

AB	Air Base
AERONET	Aerosol Monitoring Network
AFCCC	Air Force Combat Climatology Center
AFMAN	Air Force Manual
AFWA	Air Force Weather Agency
AMS	American Meteorological Society
AOR	Area of Responsibility
AP	Arabian Peninsula
AUDust	Al Udeid AB Dust
AVHRR	Advanced Very High Resolution Radiometer
CAOC	Combined (Joint and Coalition) Central Air Operations Center
CARMA	Community Aerosol Research Model from Ames/NASA
CART	Classification and Regression Tree
CENTAF	Central Command Air Forces
CENTCOM	Central Command
COAMPS	Coupled Atmosphere/Ocean Mesoscale Prediction System
DNXT	Technology Exploitation Branch
DoD	Department of Defense
DTA	Dust Transport Application
EOS	Earth Observing System
FNMOC	Fleet Numerical and Modeling Operations Center

IFR	Instrument Flight Rules
JAAWIN	Joint Air Force and Army Weather Information Network
JMP	Not an acronym, letters symbolize the statistical software
MM5	Mesoscale Model 5th generation
MODIS	Moderate Resolution Imaging Spectroradiometer
NAAPS	NRL Aerosol Analysis and Prediction System
NOGAPS	Navy Global Atmospheric Prediction System
NRL	Navy Research Lab
OEF	Operation Enduring Freedom
OIF	Operation Iraqi Freedom
OWS	Operational Weather Squadron
Pirep	Pilot Report
RMSE	Root Mean Square Error
SAGE III	Stratospheric Aerosol and Gas Experiment
SSH	Summer Shamal
SWA	Southwest Asia
TAF	Terminal Aerodrome Forecast
TM/LANDSAT	Thematic Mapper Land Satellite
TOMS	Total Ozone Mapping Spectrometer
UTC	Universal Coordinated Time
VFR	Visible Flight Rules
Z	Zulu Time

APPENDIX

Through the Linear Regression techniques discussed in great detail earlier, the JMP software derived the following linear relationships between the response and the predictors and their estimate or weighted values that the regression determined were essential to a more accurate visibility forecast.

TABLE 7. Test data set JMP derived parameter estimates

Test Parameters or Predictors	**Estimate**	**Prob>|t|**
Intercept	-119053	0.07159739
Month	-1347.08	0.00002324
Time Z	0.224984	0.37357665
WD	11.38286	0.00349545
WS KTS	-55.4148	0.05936956
WG Kts	-33.6427	0.1032988
DTA Yes	-207.482	0.54280773
NAAPS Y	-415.131	0.4485431
COAMPS Y	1260.29	2.31E-08
Sat Yes	1582.443	0.0014154
Dst Upstrm	-5519.87	0.00457463
T(C)	-161.502	2.41E-08
Td (C)	-2.01939	0.93966356
925 mb T C	-2015.32	0.00143112
925 mb Td C	-100.13	0.43100456
925 mb WS	-37.6784	0.86247388
925 mb WD	73.51254	0.00010955
850 mb T C	3160.806	0.00213658
850 mb Td C	240.6198	0.23458292
850 mb WS	77.14212	0.74323715
850 mb WD	70.49233	0.00000108
500 mb T C	-3711.49	0.00026733
500 mb Td C	-568.131	2.94E-10
500 mb WD	-63.075	0.03280659
300 mb T C	-169.912	0.02015764
300 mb WS	-188.716	0.00014466
300 mb WD	-9.37081	0.51250314
(Month-5.08609)*(WD-244.57)	9.403757	0.00622251
(Time Z-984.02)*(NAAPS Y-0.35762)	1.987093	0.00298586
(WD-244.57)*(WS KTS-12.0199)	0.488132	0.00776228
(WD-244.57)*(Dst Upstrm-0.84768)	51.79375	0.00059014
(WD-244.57)*(925 mb T C-29.0066)	39.3971	4.31E-07
(WD-244.57)*(925 mb WD-264.305)	-1.00166	2.69E-08
(WD-244.57)*(850 mb T C-23.3854)	-51.4334	0.00001293
(WD-244.57)*(850 mb Td C-0.75232)	-3.06479	0.00016697
(WD-244.57)*(850 mb WD-270.232)	-0.50401	0.03155509

Test Parameters or Predictors	Estimate	Prob>|t|
(WD-244.57)*(500 mb T C+8.01523)	43.77943	0.00025333
(WD-244.57)*(500 mb Td C+27.9298)	1.660285	0.03985711
(WD-244.57)*(500 mb WD-246.556)	0.601492	0.00865206
(WS KTS-12.0199)*(WG Kts-17.2781)	-5.26107	0.00714926
(WS KTS-12.0199)*(DTA Yes-0.12583)	-493.006	0.00002445
(WS KTS-12.0199)*(COAMPS Y-0.27152)	229.7375	0.00046302
(WS KTS-12.0199)*(Dst Upstrm-0.84768)	179.2752	0.04582129
(WS KTS-12.0199)*(925 mb T C-29.0066)	-67.3868	0.04790503
(WS KTS-12.0199)*(850 mb T C-23.3854)	57.82401	0.10682985
(WS KTS-12.0199)*(500 mb Td C+27.9298)	-10.6988	0.00006378
(WG Kts-17.2781)*(DTA Yes-0.12583)	213.8933	0.00060494
(WG Kts-17.2781)*(925 mb T C-29.0066)	113.5955	0.00036958
(WG Kts-17.2781)*(925 mb Td C-3.8543)	10.91442	0.00458294
(WG Kts-17.2781)*(925 mb WD-264.305)	-0.75336	0.0858824
(WG Kts-17.2781)*(850 mb T C-23.3854)	-120.777	0.00048916
(WG Kts-17.2781)*(850 mb WS-22.2985)	-4.06543	0.05341369
300 mb Td C	229.7776	0.03769635
Alstg	2309.713	0.29746336

TABLE 8. Validation data set JMP derived parameter estimates

Validation Parameter or Predictors	Estimate	Prob>|t|
Intercept	298977.385	0.011747
Month	18.4557721	0.983557
Time Z	0.54673813	0.161324
WD	10.4913999	0.169023
WS KTS	13.2303792	0.758333
WG Kts	-104.6832	0.00825
DTA Yes	-3483.8447	0.051086
NAAPS Y	-137.36293	0.767593
COAMPS Y	528.015307	0.233155
Sat Yes	1361.61807	0.102472
Dst Upstrm	-2727.1432	0.045528
T(C)	-34.924235	0.55191
Td (C)	-41.695016	0.45868
925 mb T C	-885.79588	0.074236
925 mb Td C	-472.05759	0.008309
925 mb WS	338.997643	0.001264
925 mb WD	-9.6283126	0.078877
850 mb T C	1129.74663	0.157707
850 mb Td C	843.593251	1.96E-05
850 mb WS	56.2956598	0.409648
850 mb WD	-20.197711	0.091346
500 mb T C	-782.72622	0.073033
500 mb Td C	-173.65196	0.021423
500 mb WD	17.5489884	0.15661
300 mb T C	-3.3112611	0.913284
300 mb WS	24.5292432	0.497193
300 mb WD	-22.016338	0.155694
(Month-5.25547)*(WD-269.343)	-15.084072	0.093607
(Month-5.25547)*(Dst Upstrm-0.65693)	-1744.0708	0.000441

Validation Parameter or Predictors	Estimate	Prob>|t|
(Time Z-969.109)*(NAAPS Y-0.40146)	2.15676417	0.006249
(WD-269.343)*(WS KTS-14.5839)	0.51025042	0.193222
(WD-269.343)*(Dst Upstrm-0.65693)	-23.513513	0.057295
(WD-269.343)*(925 mb T C-28.2073)	21.9980922	2.61E-05
(WD-269.343)*(925 mb WD-262.372)	0.08227234	0.061733
(WD-269.343)*(850 mb T C-24.1898)	-30.600183	7.73E-05
(WD-269.343)*(850 mb Td C+1.10365)	0.4394088	0.787704
(WD-269.343)*(850 mb WD-297.08)	0.10576304	0.100353
(WD-269.343)*(500 mb T C+7.43796)	12.478342	0.040998
(WD-269.343)*(500 mb WD-245.474)	-0.0182657	0.923577
(WS KTS-14.5839)*(WG Kts-21.4307)	0.09700078	0.973355
(WS KTS-14.5839)*(DTA Yes-0.11679)	-297.80019	0.118819
(WS KTS-14.5839)*(COAMPS Y-0.28467)	-76.454577	0.332701
(WS KTS-14.5839)*(Dst Upstrm-0.65693)	-87.381885	0.459338
(WS KTS-14.5839)*(925 mb T C-28.2073)	55.5830179	0.071807
(WS KTS-14.5839)*(850 mb T C-24.1898)	-58.88157	0.15336
(WS KTS-14.5839)*(500 mb Td C+30.8372)	-8.1098237	0.004785
(WG Kts-21.4307)*(925 mb T C-28.2073)	-46.455087	0.025855
(WG Kts-21.4307)*(925 mb WD-262.372)	-0.672593	0.012046
(WG Kts-21.4307)*(850 mb T C-24.1898)	56.9208504	0.054555
(WG Kts-21.4307)*(850 mb WS-17.9565)	-1.5620222	0.509202
(WG Kts-21.4307)*(925 mb Td C-3.43723)	0.91824853	0.766801
Alstg	-10950.536	0.004634
300 mb Td C	-430.76673	0.001361
(WG Kts-21.4307)*(DTA Yes-0.11679)	95.7738632	0.4343

Bibliography

Air Force Combat Climatology Center, 1957: Forecasting Visibility Restrictions Due to Dust at Dhahran Air Base in Summer, AD-161712, 4 pp.

Air Force Combat Climatology Center, 1970: Iraq and Arabian Peninsula climate and weather, NIS 30 and 32, 92 pp.

Air Force Manual (AFMAN) 15-111, *Surface Weather Observations,* 18 September 2001.

Air University Style Guide for Writers and Editors, Maxwell AFB, AL.: Air University Press, 2001, 137 pp.

American Meteorological Society, 2002: *A Brief Guide for Authors*. American Meteorological Society, Boston, MA

Barnum, B. H., N. S. Winstead, L. J. Wesley, A. Hokola, P. Colarco, O. B. Toon, P. Ginoux, G. W. Brooks, L. Hasselbarth and B. Toth, 2003: Forecasting dust storms using CARMA-dust model and MM5 weather data, [On-line at https://weather.afwa.af.mil/about_info/DTA/DTA_Tutorial.html], 16 pp.

Bukhari, S. A., 1993: Depicting dust and sand storm signatures through the means of satellite images and ground-based observations for Saudi Arabia, University of Colorado, Boulder, CO, 130 pp.

Clements, T., J. F. Mann Jr., R. O. Stone, and J. A. Eymann, 1963: A study of windborne sand and dust in desert areas, U. S. Army Tech. Rep. ES-8, 61 pp.

Fleet Numerical METOC Detachment (FNMOD) NOGAPS Climatology, 2003: Fleet Numerical Meteorology and Oceanography Detachment, Asheville, NC. [On-line at http://navy.ncdc.noaa.gov/gradsmap/indexcustomfhf.html]

Fujita, T. T., 1984: Andrews AFB microburst, SMRP Res. Paper 205, University of Chicago, IL, 38 pp.

Glickman, T. S., 2000: *Glossary of Meteorology*, 2nd Ed., American Meteorological Society, 855 pp.

Global Security, 2003: Global Security.Org, Alexandria, VA. [On-line at http://www.globalsecurity.org/military/facility/udeid.htm]

Idso, S. B., R. S. Ingram, and J. M. Pritchard, 1972: An American haboob, *Bulletin of the American Meteorological Society,* **53**, 930-935.

Lewis, L. J., and P. J. Feteris, 1989: Diagnostic study of atmospheric-terrain interaction leading to the formation of dust clouds and poor visibilities over near east desert areas, Department of Physics and Atmospheric Sciences, Jackson State University, Jackson, MS, 20 pp.

Liu, M., Walker, A. L., Westphal D. L., and Richardson, K., Dust Forecasting for Operation Iraqi Freedom, 2003: Naval Research Laboratory, Monterey, CA. [On-line at http://www.nrlmry.navy.mil/aerosol/index_frame.html]

Membery, D. A., 1983: Low level wind profiles during the Gulf Shamal, *Weather*, **38,** 18-24.

Membery, D. A., 1985: Gravity wave haboob, *Weather,* **40,** 214-221.

Miller, S. D., Hawkins, J., Turk, J., Lee, T., Richardson, K., and Kuciauskas, A., 2003: Satellite Focus: A Dynamic, Near Real-Time Satellite Resource for the DoD, The Battlespace Atmospheric and Cloud Impacts on Military Operations (BACIMO) Conference, 9-11 September 2003, Monterey, CA.

Miller, S. D., 2003: Satellite Surveillance of Desert Dust Storms, *NRL Review*, 69-77

Miner, T., 2003: Sand, dust and ash: The answer is blowing in the wind, United States Air Force *Flying Safety Magazine,* **May,** 4-7.

Mireless, M., Pederson, K., Elford, C., Reyman, M., Piasecki, J., Hosein F., Larabee, S., Williams, G., Jimenez, M., and Chapdelaine, D., 2002: Meteorological Techniques, AFWA/TN—98/002, Air Force Weather Agency, 285 pp.

Montgomery, D. C., and G. C. Runger, 2003: *Applied Statistics and Probability For Engineers*, 3rd Ed., John Wiley and Sons, Inc., New York, NY, 706 pp.

Naval Research Lab (NRL), Monterey Aerosol Page, 2003: Marine Meteorology Division, Monterey, CA. [On-line at http://www.nrlmry.navy.mil/aerosol/index_frame.html]

Neter, J., Wasserman, W., and Kutner, M. H., 1990: *Applied Linear Statistical Models Regression, Analysis of Variance, and Experimental Designs,* 3rd Ed., Homewood, IL., Irwin, 1181 pp.

Perrone, T. J., 1979: Winter Shamal in the Persian Gulf, Naval Environmental Prediction Research Facility, TR 79-06, 168 pp.

Prospero, J. M., D. M. Helgren, J. Fernandez-Partagas, and M. Estoque, 1986: Environmental conditions associated with the occurrence of large scale dust storms in arid regions of North Africa, University of Miami, Rosenthal School of Marine and Atmospheric Science, Miami, FL, 19 pp.

Rao, P. G., M. Al-Sulaiti, and A. H. Al-Mulla, 2001: Winter shamals in Qatar, Arabian Gulf, *Weather*, **56**, 444-451

Safar, M. I., 1980: Dust and duststorms in Kuwait, State of Kuwait Directorate General of Civil Aviation, Meteorological Dept., Climatological Section, 137 pp.

Salford Systems, 1995: *Data Mining with Decision Trees: An Introduction to CART®*. San Diego, CA, 133 pp.

Salford Systems, 2002: *CART® for Windows User's Guide*. San Diego, CA, 295 pp.

SAS Institute, 2003: *JMP Users Guide*. Cary, N.C. [On-line at http://web.utk.edu/~leon/jmp/default.html]

"Satellite Focus**",** Naval Research Lab (NRL), 2003: Marine Meteorology Division, Monterey, CA. [On-line at http://www.nrlmry.navy.mil/focus-bin/focus.cgi]

Siraj, A. A., 1980: Aziab weather, General Directorate of Meteorology, Saudi Arabia, 22 pp.

Wigner, K. A., and R. E. Peterson, 1982: Duststorms over Texas. Preprints, *2nd Symposium on the Composition of the Non-Urban Troposphere*, Williamsburg, VA, 52-71.

Wilkerson, W. D., 1991: Dust and sand forecasting in Iraq and adjoining countries, AWS/TN—91/001, Air Weather Service, Scott AFB, IL, 63 pp.

Wilks, D.S., 1995: *Statistical Methods in the Atmospheric Sciences,* Academic Press, San Diego, CA, 467 pp.

REPORT DOCUMENTATION PAGE

Form Approved
OMB No. 074-0188

1. REPORT DATE *(DD-MM-YYYY)*	2. REPORT TYPE	3. DATES COVERED *(From – To)*
March 2004	Master's Thesis	Jun 2003 – Mar 2004

4. TITLE AND SUBTITLE

DUST STORM FORECASTING FOR AL UDEID AB, QATAR: AN EMPIRICAL ANALYSIS

5a. CONTRACT NUMBER

5b. GRANT NUMBER

5c. PROGRAM ELEMENT NUMBER

6. AUTHOR(S)

Bartlett, Kevin S., Captain, USAF

5d. PROJECT NUMBER
None

5e. TASK NUMBER

5f. WORK UNIT NUMBER

7. PERFORMING ORGANIZATION NAMES(S) AND ADDRESS(S)
Air Force Institute of Technology
Graduate School of Engineering and Physics (AFIT/ENP)
2950 P Street, Building 640
WPAFB OH 45433-7765

8. PERFORMING ORGANIZATION REPORT NUMBER

AFIT/GM/ENP/04-01

9. SPONSORING/MONITORING AGENCY NAME(S) AND ADDRESS(ES)
Chief, Tactical Capabilities Development Attn: Capt Gerald Sullivan
HQ Air Combat Command/Weather Operations Division (HQ ACC/DOW)
205 Dodd Blvd, Ste 101 DSN: 574-8442
Langley AFB, VA 23665-2789 e-mail:Gerald.Sullivan@langley.af.mil

10. SPONSOR/MONITOR'S ACRONYM(S)

11. SPONSOR/MONITOR'S REPORT NUMBER(S)

12. DISTRIBUTION/AVAILABILITY STATEMENT
APPROVED FOR PUBLIC RELEASE; DISTRIBUTION UNLIMITED.

13. SUPPLEMENTARY NOTES

14. ABSTRACT

Dust storms are extreme weather events that have strong winds laden with visibility reducing and operations limiting dust. The Central Command Air Forces (CENTAF) 28th Operational Weather Squadron (OWS) is ultimately responsible for forecasting weather in the vast, data denied region of Southwest Asia in support of daily military and humanitarian operations. As a result, the 28th OWS requests a simplified forecasting tool to help predict mesoscale dust events that affect coalition operations at Al Udeid AB, Qatar. This research satisfies the 28th OWS request through an extensive statistical analysis of observational data depicting seasonal dust events over the past 2 years. The resultant multiple linear regression best fit model combines 28 easily attainable model outputs, satellite imagery, surface and upper air observations, and applies a linear transformation equation. The model provides the end user with a numerical visibility prediction for Al Udeid AB that is verified against a seasonally divided and independent validation data set that yields an R^2 of 0.79 while maintaining < 800 m accuracy. The operational significance of the summarized seasonal patterns and dust storm type offers operators within the region a quick synopsis of possible dust prone periods and duration of events; whereas the best Fit Model offers an easy-to-use, accurate dust forecasting tool. The Fit Model developed is ready to use and is expected to positively affect weather forecasts for flight operations at Al Udeid AB.

15. SUBJECT TERMS
Dust storms, dust storm forecasting, Qatar weather, Al Udeid AB weather, Persian Gulf weather

16. SECURITY CLASSIFICATION OF:			17. LIMITATION OF ABSTRACT	18. NUMBER OF PAGES	19a. NAME OF RESPONSIBLE PERSON
a. REPORT	b. ABSTRACT	c. THIS PAGE			Steven T. Fiorino, Maj USAF (ENP)
U	U	U	UU	103	19b. TELEPHONE NUMBER *(Include area code)* (937) 255-3636 x4506 e-mail: steven.fiorino@afit.edu

Standard Form 298 (Rev. 8-98)
Prescribed by ANSI Std. Z39-18